Oxidative steam reforming of glycerol. A review

Rui Moreira[*] [(1)], Fernando Bimbela [(2)], Luis M. Gandía [(2)], Abel Ferreira [(1)], Jose Luis Sánchez [(3)], António Portugal [(1)†]

[(1)] University of Coimbra, CIEPQPF, FCTUC, Department of Chemical Engineering, Rua Sílvio Lima, Pólo II – Pinhal de Marrocos, 3030-790 Coimbra, Portugal

[(2)] Grupo de Reactores Químicos y Procesos para la Valorización de Recursos Renovables, Institute for Advanced Materials and Mathematics (InaMat^2), Universidad Pública de Navarra, Pamplona, Spain

[(3)] Thermochemical Processes Group (GPT), Aragón Institute for Engineering Research (I3A), Universidad de Zaragoza, Spain

Abstract:

This review article presents the state-of-the-art on the catalytic oxidative steam reforming (OSR) of glycerol to produce syngas. Concerning the different technologies proposed for the catalytic OSR of glycerol, the following key points can be highlighted: (1) the robustness is much higher than other reforming technologies, (2) several catalysts can work with low deactivation, some of which can recover almost full activity by suitable regeneration, (3) syngas production by catalytic OSR of glycerin is higher than with concurrent technologies, (4) their scaling-up remains an unrealized task, (5) the thermodynamics of the process has been sufficiently covered in the literature, (6) there is a significant lack of kinetic and mechanistic studies that could help gaining deeper insight on the process, (7) novel concepts and reactor designs must be proposed for their development at larger scales, (8) new catalyst formulations must be developed for attaining higher resistance against oxidation and (9) process intensification could help developing them at larger scales.

[*] Corresponding author: Rui Moreira (ruimoreira@eq.uc.pt).
[†] Deceased on January 11th, 2021.

Highlights:

1. The robustness of OSR of glycerol is much higher than other reforming technologies.
2. Several catalysts can work with low deactivation caused by carbon deposits.
3. The production of syngas by OSR is high in comparison with concurrent technologies.
4. Excellent results at lab scale, though the scale-up of OSR of glycerol is missing.

Keywords: Glycerin, autothermal reforming, syngas, oxidative steam reforming, structured catalytic reactors

Word count: 10,439 words

NOMENCLATURE:

Abbreviations: APR - aqueous phase reforming; **ASU** - air separation units; **ATR** - autothermal reforming; **CAPEX** - capital expenditure; **CG** - crude glycerol (or crude glycerin); **EDS** - energy-dispersive X-ray spectroscopy; **ER** - Eley-Rideal; **EU** - European Union; **FAO** - Food and Agriculture Organization; **FFA** - free fatty acids; **G –** glycerol (or glycerin); **GHG** - greenhouse gas: **LH** - Langmuir-Hinshelwood; **LHHW** - Langmuir-Hinshelwood-Hougen-Watson; **LHV –** Lower Heating Value; **MTE** - methanol to ethylene; **MTG** - methanol to gasoline; **MTO** - methanol to olefins; **MTP** - methanol to propylene; **OECD** - Organization for Economic Cooperation and Development; **OPEX** - operational expenditure; **OSR** - oxidative steam reforming; **P2G** - power to gas; **PEMFC** - proton exchange membrane fuel cells; **PO** - partial oxidation; **PPI** - pores per inch; **PRSV** - Peng-Robinson Sryjek-Vera; **ScWR** - supercritical water reforming; **SEM** - scanning electron microscopy; **SERS –** sorption enhanced steam reforming; **SR** - steam reforming; **TPO** - temperature programmed oxidation; **WGS** - water gas shift; **WtE –** Waste-to-Energy.

Process variables: $\mathbf{C_{p,steam}}$ **–** specific heat at constant pressure ($J \cdot mol^{-1} \cdot K^{-1}$); $\mathbf{E_a}$ - activation energy ($kJ \cdot mol^{-1}$); **GHSV** - gas hourly space velocity (h^{-1}); $\mathbf{H_2/CO}$ **–** hydrogen to carbon monoxide molar ratio (mol/mol); **K** - adsorption equilibrium constant; $\mathbf{k_0}$ - Arrhenius-type pre-exponential factor or frequency factor ($mol\ C \cdot g_{cat}^{-1} \cdot min^{-1} \cdot atm^{-3.5}$); **O/C –** elemental oxygen to carbon molar ratio (mol/mol); **O/CG –** elemental oxygen to crude glycerol molar ratio (mol/mol); **O/G** - elemental oxygen to glycerol molar ratio (mol/mol); $\mathbf{O_2/C}$ **–** molecular oxygen to carbon molar ratio (mol/mol);

O_2/CG – molecular oxygen to crude glycerol molar ratio (mol/mol); **O_2/G –** molecular oxygen to glycerol molar ratio (mol/mol); **S/C –** steam to carbon molar ratio (mol/mol); **P –** pressure (MPa); **S/CG –** steam to cure glycerol molar ratio (mol/mol); **S/G –** steam to glycerol molar ratio (mol/mol); **T –** temperature (K); **TOF** - turnover frequency; **W/F_{A0} –** mass of catalyst per mol of carbon (or glycerol) fed per minute ($g_{cat}\cdot min\cdot mol^{-1}$); **WHSV** - weight hourly space velocity (h^{-1} or $ml/g_{cat}\cdot min^{-1}$); **ΔH^o** - enthalpy of formation ($kJ\cdot mol^{-1}$); **ΔH^o_{vap}** - enthalpy of vaporization ($kJ\cdot mol^{-1}$).

1. Introduction

The European Union (EU) legislation demands that at least 10% of biofuels should be mixed in transportation diesel by 2020. Of those, 7% can be fulfilled by first generation biodiesel (produced from virgin vegetable oil), 2.5% can be attained by biodiesel produced from waste vegetable oil and animal grease, and 0.5% should be met by advanced biofuels [1–4]. Figure 1 shows the evolution and the prospects for the biodiesel market according to the database compiled by the Organization for Economic Cooperation and Development (OECD) and the Food and Agriculture Organization (FAO) database [5].

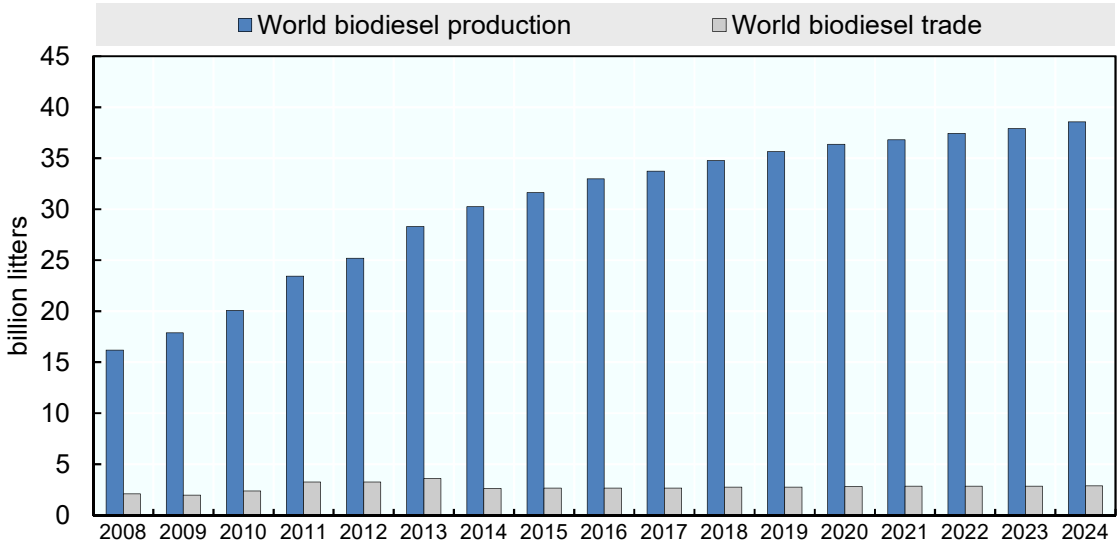

Figure 1 - Time evolution for world biodiesel market (2008-2015) and projected evolution (2015-2024) [5].

In the very recent update of OECD/FAO's report [6], prospects for the next decade indicate that world biodiesel production and consumption will continue to grow, even though at a lower rate. Global demand for vegetable oil is expected to increase up to more than 28 million tons by 2028. Biodiesel is a mixture of methyl or ethyl esters produced by the transesterification (Equation 1) of lipids, which are long chain (C_8-C_{24}) carboxylic acids bonded to a glycerol (or glycerin, $C_3H_8O_3$) molecule [7–9].

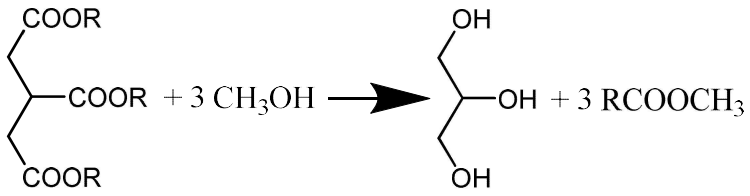

(Eq.1)

A byproduct stream is obtained usually defined as crude glycerol (CG), as opposed to the pure chemical glycerol (G). CG can be purified (by distillation) into technical grade glycerin, which can be used as reagent in different industries, including the food industry, cosmetics, and pharmaceuticals [10–12]. Figure 2 shows some chemicals that can be obtained from glycerin.

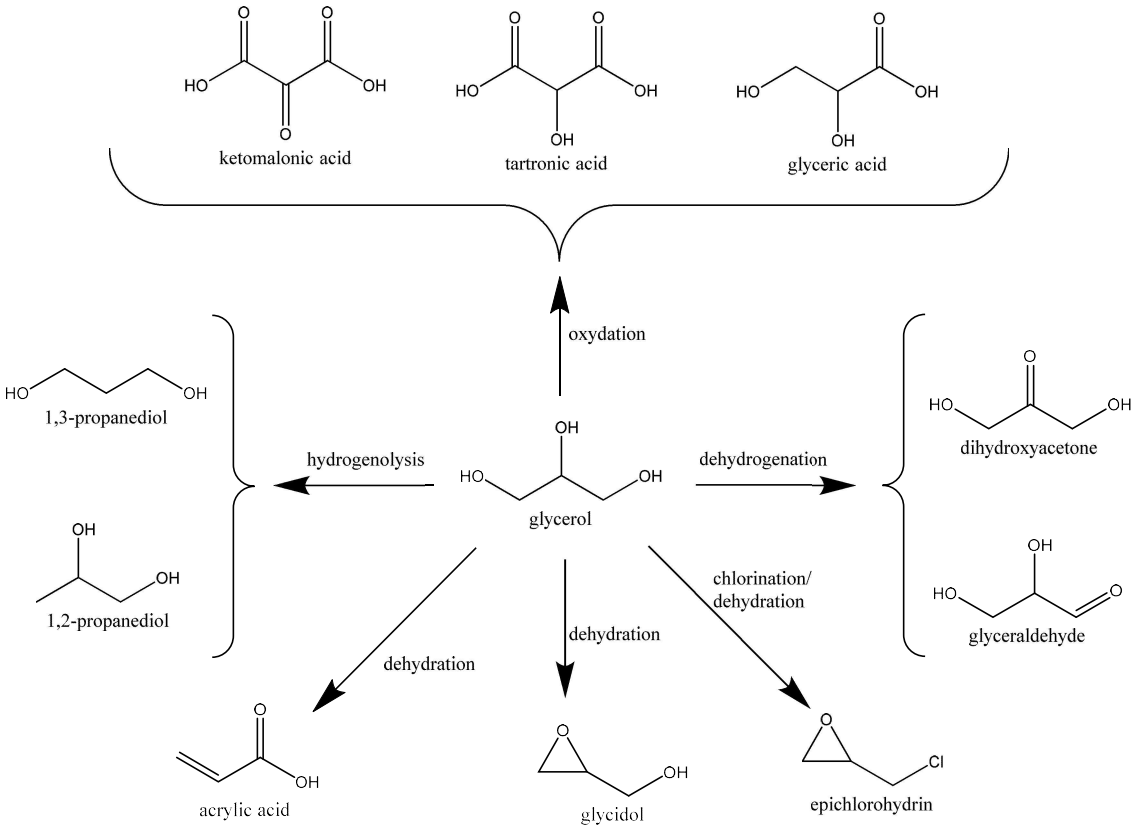

Figure 2 – Routes for glycerol transformation into higher value-added chemicals.

World glycerol production in 2012 was around 2 million tons, with increase expectations of 6% per annum between 2012 and 2018 [10,13], which led to lower prices as the biodiesel production increased. CG typically reduced its price in different world markets from around 400 US$/ton in 2001 to roughly 100 US$/ton in 2011, and some US biodiesel producers were forced at times to sell it for 44 US$/ton or less [14]. The surplus glycerin that has flooded the world market in the

last 20 years cannot be accommodated by its present demand in different industrial applications. Thus, many researchers started seeking for new ways for exploiting glycerol by converting it into higher value-added chemicals and products.

2. Thermochemical valorization of glycerol

Thermochemical valorization of glycerol aims the production of valuable chemicals and fuels by different high-temperature (473–1273 K) processes. Different strategies can be adopted for its valorization within the context of Waste-to-Energy (WtE) technologies [15]. The straightforward use of CG as a fuel by direct combustion could be considered as a simple way to increase the sustainability of the biodiesel supply chain [16]. However important issues (such as its poor LHV, ineffective combustion [17], large concentrations of fly ash with high alkali metal content [18], emissions of very toxic pollutants such as acrolein [19], and technical challenges of atomization in combustion engines [16] and boilers [18]) make this valorization route non-viable at the moment. Furthermore, it would represent a low added value application of this resource and, therefore, other alternatives should be first considered.

Alternatively, glycerol can be converted into synthesis gas (in short, syngas), which is a mixture of H_2 and CO of great industrial interest. Syngas can be used as feedstock to produce virtually any organic chemical. For instance, syngas can be converted into synthetic hydrocarbons by Fischer-Tropsch technologies. An interesting application of glycerin-derived syngas is the production of methanol, which can be used as a solvent, as an intermediate for producing different oxygenates (*e.g.*, formaldehyde [20,21], formic acid [22], acetic acid [23] and dimethyl ether [24]), in the manufacturing of biodiesel itself or in methanol-to-hydrocarbons processes (*e.g.*, methanol-to-ethylene, MTE, methanol-to-gasoline, MTG, methanol-to-olefins, MTO, and methanol-to-propylene, MTP, methanol-to-aromatics, MTA) [25–27]. A possible biodiesel process scheme including glycerol valorization via syngas is shown in Figure 3.

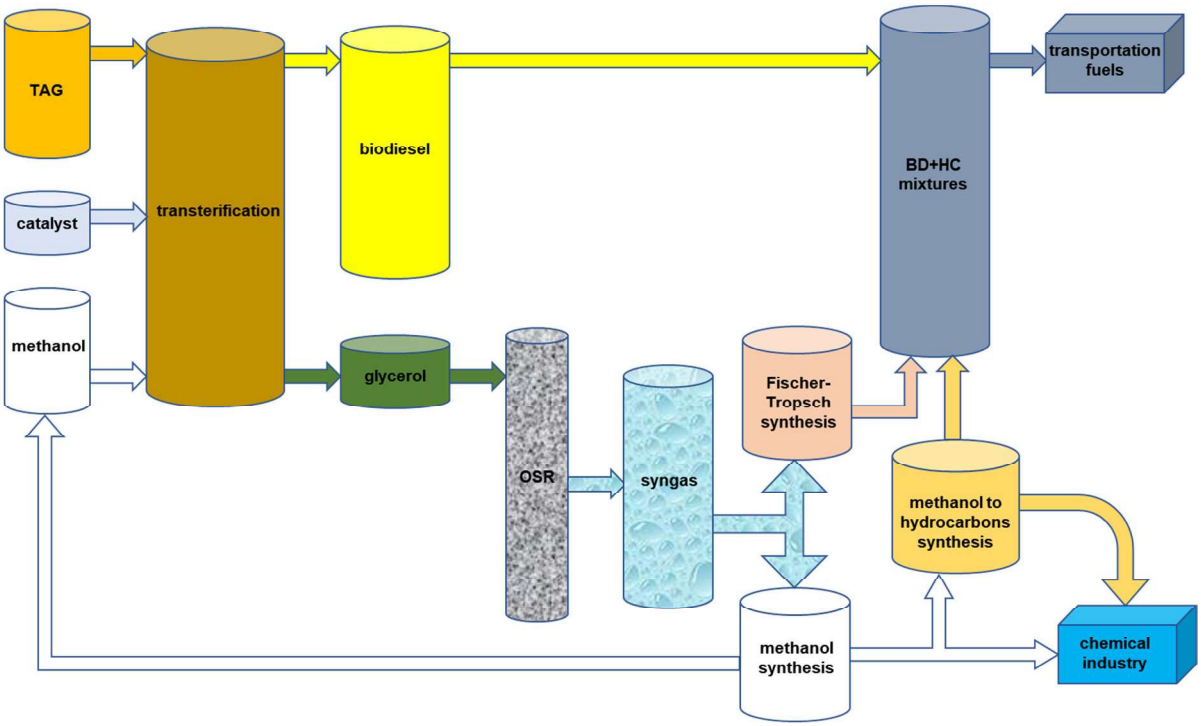

Figure 3 – Main routes of glycerin valorization by by oxidative steam reforming (OSR) (BD – biodiesel; HC – hydrocarbons).

Several thermochemical routes can generate syngas and other valuable chemicals from glycerin, such as hydrothermal gasification, which could be divided into aqueous phase reforming (APR), and supercritical water reforming (ScWR), depending on the use of hot compressed water under subcritical or supercritical conditions. Alternatively, syngas can by produced from glycerol by pyrolysis, partial oxidation (PO), steam reforming (SR), autothermal reforming (ATR) and oxidative steam reforming (OSR). The most widely studied route is hydrogen production via catalytic SR because it is a well-established technology in the industry, and over 95% of present world hydrogen production is accomplished by SR of fossil resources [28]. Renewable hydrogen production is a topic that has gained renewed interest in recent years, to meet the anticipated short and mid-term increase in hydrogen demand. Moreover, new targets and strategic plans have been adopted by various countries, related to the development of hydrogen fuels and fuel cells [29]. High-purity hydrogen production by steam reforming of glycerol has been addressed, either in combination with the use of membrane technologies or with adsorbents to capture CO_2, a process known as sorption enhanced steam reforming (SERS) [30]. Processes for valorizing other biomass streams such as lignin-derived bio-oil hydrodeoxygenation can benefit from

147 sustainable *in situ* hydrogen generation by steam reforming of different feedstocks, including
148 glycerol among others [31]. Very recently, some authors have proposed dry reforming of glycerol
149 to produce syngas, which could constitute a route for valorizing CO_2. Mini-reviews on this topic
150 can be found in the literature [32,33]. Novel routes for syngas production from glycerol, including
151 thermal arc plasma [34] or photocatalytic splitting of glycerol into methanol and syngas [35] have
152 been proposed in recent years.
153 Table 1 summarizes the main differences and advantages of the above commented
154 thermochemical processes for valorizing glycerol into hydrogen and syngas.
155

156 Table 1 –Comparison of main thermochemical processes for glycerol valorization.

Process	Conditions	Characteristics
Aqueous-phase reforming	Low temperature (493-553 K). High pressure (3-8 MPa). Uses liquid H_2O as reactant.	Does not require energy to vaporize water. Produces H_2 with high-purity (high H_2/CO ratio). Low temperatures favor the WGS reaction. Requires post-separation of large amounts of CO_2. Requires longer reaction times and gives lower selectivity to H_2 compared to to SR (alkanes formed in side reactions: methanation, Fischer-Tropsch and glycerol dehydration). Catalysts deactivate fast by coke deposition. Depends on noble metals to attain acceptable conversion levels and stable operation. Has not attained economic feasibility due to low productivities and the need to first remove impurities from the crude glycerol.
Supercritical reforming	Moderate reaction temperature (≥673 K). High pressure (≥22.1 MPa). Uses supercritical H_2O as reactants.	High temperature (>873K) and pressure (>25 MPa) are needed for high conversion. It is mainly oriented to H_2 production. Different catalysts are used to improve conversion and yield.
Pyrolysis	Moderate reaction temperature (773-1072 K). Atmospheric pressure. Uses inert atmosphere (usually N_2).	It is mainly oriented to syngas production. Requires external heating. Can be operated with or without catalyst.
Steam reforming	Moderate reaction temperature (823-1123 K). Atmospheric pressure. Uses H_2O as reactant.	It is mainly oriented to H_2 production (high H_2/CO ratio). Requires significant external energy to vaporize and heat water, and for endothermal reactions. Requires post-separation of large amounts of CO_2. Catalysts deactivate fast mainly by graphitic carbon. Steam and dry reforming of CH_4 can occur.

Dry reforming	Moderate reaction temperature (≃773 K). Atmospheric pressure. Uses CO_2 as reactant.	It is mainly oriented to syngas production (low H_2/CO ratio). Uses CO_2 as reactant. The increase of CO_2/G ratio improves the catalysts stability (reduces the deposition of carbonaceous species on the catalyst). Requires significant external energy for endothermal reactions. Side reaction can lead to the formation of side products (e.g., acetaldehyde, alkanes, alcohols, acetone, ethylene, acetic acid and acrolein). Catalysts deactivate fast mainly by coke accumulation.
Partial oxidation	High reaction temperature (>1273 K). Atmospheric pressure. Uses O_2/air as reactants.	Hight temperature can lead to catalyst sintering. Difficult to control (hotspots may occur in the catalyst) - formation of side products. Does not require additional external heat. Selectivity depends on oxygen partial pressure. Exhibits low coke formation.
Autothermal reforming	High temperature (900-1173 K). Atmospheric pressure. Uses O_2/air and H_2O as reactants.	Process heat is obtained by consumption of glycerol (oxidation reactions). Produced low H_2 and syngas yields. Does not require external heat. Reaction temperature can be optimized by reactants composition adjustment. Exhibits catalyst deactivation (mainly amorphous carbon).
Oxidative steam reforming	Moderate reaction temperature (823-1123 K). Atmospheric pressure. Uses O_2/air and H_2O as reactants.	Requires little-to-none external energy for endothermal reactions. Exhibits catalyst deactivation (mainly amorphous carbon).

157

158

APR and ScWR are mainly oriented to the production of hydrogen from organics. APR has the advantage that it produces high-purity hydrogen (very low CO concentration) at high pressure (3-8 MPa) and low temperature (493-553 K). However, APR requires longer reaction times and has lower selectivity to hydrogen in comparison to SR, and the process yield relies on the use of catalysts [13,36]. APR catalysts usually deactivate fast (by coke deposition) or depend on expensive noble metals to attain acceptable conversion levels and stable operation during reasonable operating times. This has hindered any attempts to scale-up the technology beyond the usual micro-scale and bench-scale laboratory setups. Furthermore, H_2 produced at APR conditions is thermodynamically unstable and is quickly consumed in alkane formation, via methanation and Fischer-Tropsch reactions [37]. Low selectivity and moderate hydrogen yields together with very low space velocities and catalyst deactivation, should lead researchers to focus on APR liquid products rather than on hydrogen production. In particular, large amounts of ethylene glycol and propylene glycol are typically produced by catalytic APR of glycerol. In contrast, high hydrogen yields can be obtained by ScWR at temperatures >873 K; while temperatures <723 K favor methane formation [13,36]. The need for high temperatures and high pressures as well as the inherent problems of high corrosiveness (caused by supercritical water onto the equipment) make ScWR economically unattractive [13,36].

SR of glycerol can be broadly described by two main reactions: pyrolysis and water-gas shift (WGS) reaction. In SR, glycerin is first thermally decomposed into syngas by pyrolysis (Eq. 2). Syngas composition is then adjusted by the WGS reaction (Eq. 3), converting CO into CO_2 and H_2 [13].

If glycerin were fully converted into syngas, the stoichiometry would be described by Equation 4. However, since the WGS is an equilibrium reaction, unpractical amounts of steam would be required to achieve full conversion of CO, thus SR is better described by Equation 5 [13].

$$C_3H_8O_3 \rightarrow 3\ CO + 4\ H_2,\ \Delta H^0 = +251\ kJ{\cdot}mol^{-1} \quad \text{(Eq.2)}$$

$$CO + H_2O \leftrightarrow H_2 + CO_2,\ \Delta H^0 = -41\ kJ{\cdot}mol^{-1} \quad \text{(Eq.3)}$$

189 $C_3H_8O_3 + 3\ H_2O \rightarrow 3\ CO_2 + 7\ H_2$, $\Delta H^0 = +128\ kJ \cdot mol^{-1}$ (Eq.4)

190

191 $C_3H_8O_3 + \alpha\ H_2O \rightarrow (3-\alpha)\ CO + \alpha\ CO_2 + (4+\alpha)\ H_2$, $\Delta H^0 = 251 - (41 \cdot \alpha)\ kJ \cdot mol^{-1}$, $(0 \leq \alpha \leq 3)$ (Eq.5)

192

193 As can be seen by the reaction enthalpies (Eqs. 2-4), SR is a very energy-intensive process due
194 to the endothermicity of the involved reactions [13]. Moreover, significant energy is necessary to
195 vaporize water ($\Delta H°_{vap}$=41 $kJ \cdot mol^{-1}$) and heat it up to relevant reaction temperatures
196 ($C_{p,steam}$=37.47 $J \cdot mol^{-1} \cdot K^{-1}$ at 373 K), typically in the range of 823-1123 K. In allothermal SR
197 processes, an external energy source must supply the necessary heat for sustaining operation
198 inside the SR unit.
199 Other reactions may play important roles during SR, such as the reaction of glycerin with
200 hydrogen (Eq. 6) and carbon dioxide (Eq.7), wet (Eq. 8) and dry (Eq. 9) reforming of methane, as
201 well as reactions that contribute to carbon formation (Eqs. 10-13) [28].

202

203 $C_3H_8O_3 + 2\ H_2 \leftrightarrow 2\ CH_4 + CO + 2\ H_2O$, $\Delta H^0 = -167\ kJ/mol$ (Eq.6)

204

205 $C_3H_8O_3 + CO_2 \leftrightarrow H_2O + 4\ CO + 3\ H_2$, $\Delta H^0 = +292\ kJ/mol$ (Eq.7)

206

207 $CH_4 + H_2O \leftrightarrow 3\ H_2 + CO$, $\Delta H^0 = +206\ kJ/mol$ (Eq. 8)

208

209 $CH_4 + CO_2 \leftrightarrow 2\ H_2 + 2\ CO$, $\Delta H^0 = +247\ kJ/mol$ (Eq. 9)

210

211 $CH_4 \rightarrow 2\ H_2 + C$, $\Delta H^0 = +75.6\ kJ/mol$ (Eq. 10)

212

213 $CO + H_2 \leftrightarrow H_2O + C$, $\Delta H^0 = +131\ kJ/mol$ (Eq. 11)

214

215 $2\ CO \leftrightarrow CO_2 + C$, $\Delta H^0 = +172\ kJ/mol$ (Eq. 12)

216

217 $CO2 + H_2 \leftrightarrow 2\ H_2O + C$, $\Delta H^0 = +90\ kJ/mol$ (Eq. 13)

In contrast, glycerol combustion (Equation 14) is an exothermal process, which presents several drawbacks, as previously mentioned [19].

$$C_3H_8O_3 + 7/2\ O_2 \rightarrow 3\ CO_2 + 4\ H_2O,\ \Delta H^0 = -1565\ kJ\cdot mol^{-1} \quad \text{(Eq.14)}$$

More interestingly, partial oxidation (PO) allows the exothermal conversion of glycerol into H_2 and CO_2, and no water evaporation is needed [13,36,38]. By feeding different sub-stoichiometric amounts of O_2, syngas can be obtained by PO of glycerol, as described by Equations 15-18 [13,36,38].

$$C_3H_8O_3 + 1/2\ O_2 \rightarrow 2\ CO_2 + 4\ H_2,\ \Delta H^0 = -31\ kJ\cdot mol^{-1} \quad \text{(Eq.15)}$$

$$C_3H_8O_3 + O_2 \rightarrow CO + 2\ CO_2 + 4\ H_2,\ \Delta H^0 = -315\ kJ\cdot mol^{-1} \quad \text{(Eq.16)}$$

$$C_3H_8O_3 + 3/2\ O_2 \rightarrow 3\ CO_2 + 4\ H_2,\ \Delta H^0 = -598\ kJ\cdot mol^{-1} \quad \text{(Eq.17)}$$

$$C_3H_8O_3 + (3-\alpha)/2\ O_2 \rightarrow \alpha\ CO + (3-\alpha)\ CO_2 + 4\ H_2,\ \Delta H^0 = -598+(283\cdot\alpha)\ kJ/mol,\ (0\leq\alpha\leq 3) \quad \text{(Eq.18)}$$

Heat control and H_2 production can be improved by oxidative steam reforming (OSR) [13]. The OSR can be seen as a combination of PO and SR (Eqs. 19-20) [13,36,38].

$$C_3H_8O_3 + 3/4\ O_2 + 3/2\ H_2O \rightarrow 3\ CO_2 + 11/2\ H_2,\ \Delta H^0 = -240\ kJ\cdot mol^{-1} \quad \text{(Eq.19)}$$

$$C_3H_8O_3 + (3/4-\alpha)\ O_2 + (3/2-\gamma)\ H_2O \rightarrow [(3-(2\cdot\alpha+\gamma)]\ CO_2 + (2\cdot\alpha+\gamma)\ CO + (11/2-\gamma)\ H_2,\ \Delta H^0 = -532 + (566\cdot\alpha) + (261\cdot\gamma)\ kJ\cdot mol^{-1},\ (0\leq \alpha \leq 3/4\ ;\ 0\leq \gamma \leq 3/2) \quad \text{(Eq.20)}$$

To achieve self-sustained operation (autothermal reforming, ATR), the heat released in the reaction (Equation 20) must be higher than zero, *i.e.*, sufficient heat must be generated for carrying out the endothermic reactions (glycerol pyrolysis and steam reforming), for sustaining the operating temperature inside the reactor, and to overcome all the energy loses in the

248 reforming unit. This can be accomplished by carefully controlling the O_2 fed into the reactor. Thus,
249 to achieve the maximum yield of syngas the theoretical values of α and ɣ should be ca. 3/5 and
250 ca. 5/7, respectively [13]
251 Compared to SR, much less research has been dedicated to OSR of glycerin. This process could
252 allow for high efficiency and compactness of gasification systems, and may turn possible the
253 development of small scale units for decentralized autonomous production of syngas [36]. By
254 balancing the amounts of oxygen and steam, syngas and heat can be obtained in such a way that
255 the process can be conducted autothermally without needing any additional external energy input
256 [13,36,38].
257 Coke deposition on catalysts is lower in OSR in comparison to SR, thus enabling longer time-on-
258 stream operation, but reactive beds containing catalysts are difficult to control and hot spots can
259 occur due to the exothermicity of the PO reactions [13]. This can lead to sintering issues that
260 would gradually cause catalyst deactivation and activity loss. In addition, oxidizing atmospheres
261 may cause certain catalysts based on non-noble transition metals to easily reoxidize upon
262 exposure to gas-phase oxygen [39]. Oxidized transition metals may promote complete
263 combustion instead of catalytic PO, and eventually lead to totally ceasing catalytic reactions and
264 syngas production [40]. In these processes, both oxygen and steam are simultaneously fed into
265 the reactor. Feeding steam helps increasing hydrogen production, whilst feeding
266 substoichiometric oxygen (with respect to complete combustion) allows for glycerol PO, thus
267 supplying heat for the endothermal reactions [13,36,38].
268 The development of OSR technologies for producing syngas from natural gas was pioneered by
269 Haldor Topsøe [41]. Full scale OSR technologies (or OSR working in autothermal regime) using
270 natural gas as feedstock have reached the maturity level since the late 1950's, when the first OSR
271 plants were commissioned for ammonia synthesis. More recently, OSR was further developed for
272 producing synthesis gas and hydrogen from natural gas, and various companies offer full-scale
273 technologies based on OSR units. Full-scale OSR processes usually rely on sequential, separate
274 PO and catalytic SR reactors, or combine both processes in a single reactor unit while maintaining
275 the same reactive sequence (non-catalytic PO followed by SR). An example of this concept is
276 Topsøe's SynCOR^{TM} technology for producing syngas, the schematic diagram of which is
277 presented in Figure 4, together with a schematic close-up view of the single-unit reactor.

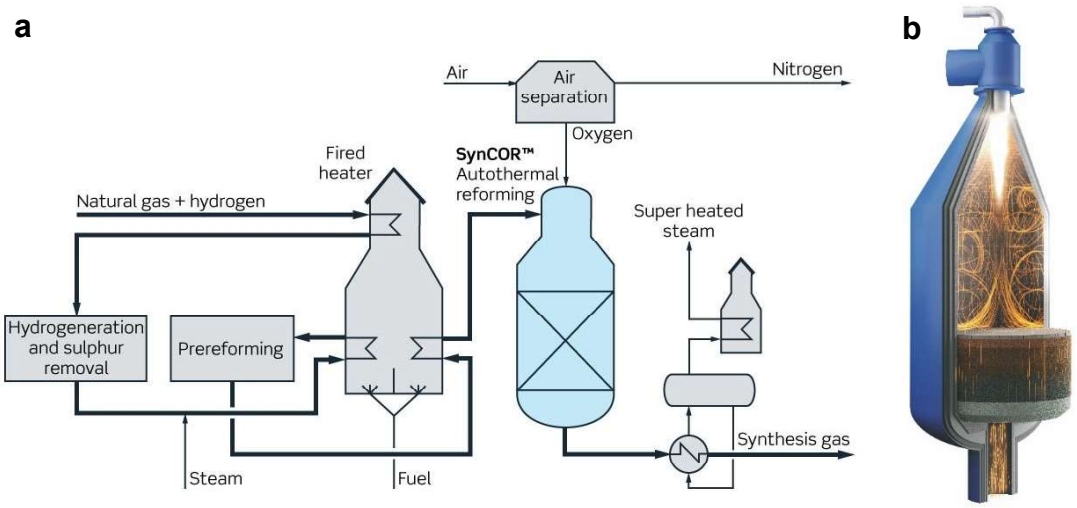

Figure 4 - Topsøe's SynCOR^{TM} technology: (a) schematic diagram of the syngas plant and (b) schematic view of the reactor. (Images used as authorized by the Haldor Topsøe with all rights reserved [42]).

A similar concept was presented by Dybkjaer for methanol production [43]. These full-scale technologies include dedicated air separation units (ASU) built onsite to feed pure O_2 into the OSR reactor. The ASU requires important capital investments, which can represent up to 40% of the costs of a large-scale synthesis gas plant [43]. Alternative operation using compressed air is possible in schemes that do not recycle the product gas, so as to avoid high accumulation of N_2 [44]. However, this limits its technoeconomic feasibility and subsequent application in plants having very large capacities. Other setbacks of using air instead of pure O_2 include big purge gas streams and substantial additional costs involved in compressing air.

All the OSR concepts and technologies presented above could constitute a good opportunity and a starting point for developing alternative technologies based on glycerol. However, more efforts are needed to scale-up any proposed OSR technology using glycerol. To date, the existing literature only presents laboratory-scale proofs-of-concept [45–48] or purely theoretical simulation studies [49–51]. In addition, studies concerning the techno-economic assessment of large-scale syngas production by glycerol OSR should be conducted for an effective scale-up of any proposed

299 technology, with particular focus on the use of compressed air or pure O_2 as alternatives for the
300 oxidizing agent.
301
302 **3. Thermodynamics of oxidative steam reforming of glycerol**
303 Several studies have analyzed the OSR of glycerol from the thermodynamic point of view. The
304 pioneering work was that by Wang *et al.* [52], who performed equilibrium calculations by
305 minimizing Gibbs free energy. From the thermodynamic point of view, raising the reaction
306 pressure has a detrimental effect on the overall OSR reaction, which is why the thermodynamic
307 studies in the literature rule pressure out and all simulations are conducted at atmospheric
308 pressure. Therefore, one question that remains unanswered is whether it could be better to have
309 a trade-off between the penalty on syngas production caused by increasing the pressure, and the
310 energy saved by avoiding pressurization of the produced syngas for further downstream operation
311 (*e.g.*, Fischer-Tropsch or methanol synthesis). Depending on the process configuration, it could
312 be better to pressurize the OSR reactor and obtain syngas at the required pressure for the
313 selected downstream application, at the expense of decreased syngas production. This would be
314 an interesting point to analyze in further technoeconomic assessment studies.
315 In general, the effect of the reaction temperature on the thermodynamic equilibrium follows the
316 same trends as those found in the SR of oxygenates and hydrocarbons. This is somewhat
317 anticipated, because the strong endothermic nature of the glycerol SR and pyrolysis reactions
318 (Eqs. 19-20) play a significant role in the overall OSR reaction. The addition of controlled amounts
319 of oxygen is thus affecting mostly the selectivity to products because the idea is to have PO of
320 the glycerol feed, only in the necessary amount to make the overall OSR reaction self-sustained
321 energy-wise. Therefore, based on the existing knowledge in the field of SR of oxygenates, one
322 can expect optimal temperatures for maximized hydrogen production around 923 K and S/C ratios
323 around 3 (operating at atmospheric pressure) [53–55]. These would represent reference values
324 that should be carefully adjusted depending on two basic parameters that are somehow
325 interconnected: the steam to carbon ratio (S/C) and the oxygen to carbon ratio (O/C).
326 Nonetheless, the final choice of the optimized operating parameters may not only be based on
327 thermodynamic aspects, but also on other important factors for the process, such as avoiding
328 carbon deposition on the catalyst or re-oxidation of the catalytic active phase.

In Wang *et al.* [52], the thermodynamic analysis was done considering the influence of the main operating parameters on the equilibrium compositions: the reaction temperature, the steam-to-glycerol molar ratio and the oxygen-to-glycerol molar ratio. The most favorable conditions for hydrogen production were achieved at T=896-1000 K, S/G=9-12 (*i.e.*, S/C=3-4) and O/G=0.0-0.4 (*i.e.,* O/C=0-1.2) [52]. Moreover, thermoneutral conditions (when using S/G=9-12) were obtained at O/G of ≃0.36 at 896 K and 0.38-0.39 at 1000 K. Under such autothermal conditions, the maximum number of moles of hydrogen produced per mole of glycerol was 5.62 at 896 K and 5.43 at 1000 K with a S/G=12, whilst negligible methane and carbon formation can be theoretically attained. Conversely, at 700-900 K the maximum CO production was obtained at S/G=1 and O/G= 0.6-1.8, whereas at 1000 K the CO production was maximized at S/G=1 and O/G=0. Almost no CH_4 formation was observed with S/G>7, O/G>2.2 at 900 K, as well as with S/G>6, O/G>1.2 at 1000 K. No carbon formation took place in the entire considered ranges of S/G and O/G at 1000 K, at 900 K carbon was produced only when O/G<0.4 (S/G=1) and O/G=0 (S/G=2), and for other temperatures low water and oxygen contents in the feed favored the formation of more coking [52].

Authayanun *et al.* [56] reported a thermodynamic study on the OSR of CG for hydrogen production using HYSYS software. CG was modelled by mixtures of methanol and glycerol at four different mole fractions (40-100%), but other impurities typically found in CG were not considered. The presence of methanol in the CG mixture caused lower H_2 and CO yields as compared to pure glycerol. Oxygen-to-CG molar ratios (O/CG) ranging between 0.4 and 0.7 were proposed for OSR of CG depending on its purity. However, this ratio should be increased with increasing S/C ratios and methanol content in the feed.

Yang *et al.* also conducted a thermodynamic study of the OSR of glycerol using Aspen Plus software [57]. Graphite carbon was included in the list of possible products, and the minimization of the total Gibbs free energy was carried out. The equilibrium selectivity to hydrogen was 86% at 923 K, S/C=2 and C/O=1. Carbon-free operation was thermodynamically favored when the reaction temperature was increased, whilst simultaneously increasing the S/C and the O/C ratios. A trade-off between H_2 yield and energy consumption must be achieved by selecting adequate S/C and O/C ratios, and the reaction temperature should be in the range of 873-973 K. To obtain

358 the maximum of hydrogen yield under the OSR condition, the C/O ratio should be in the 0.8-1.2
359 range, which basically corroborates the result obtained in the study by Wang *et al.* [52].
360 Hajjaji *et al.* [58] conducted energy and exergy analyses of the OSR of glycerol. First, they
361 developed a thermodynamic study based on the minimization of the total Gibbs free energy using
362 Aspen Plus. Then, energy and exergy analyses were developed for the entire OSR process,
363 aiming for hydrogen-rich syngas to be used in hydrogen proton exchange membrane fuel cells
364 (PEMFC). The thermal efficiency of the simulated OSR process was 66.6%, *i.e.,* approximately
365 two-thirds of the energy fed into the process are recovered in the useful product (H_2) whilst the
366 rest is exhausted in the off-gas. The exergy efficiency of the OSR base-case process was 57%,
367 and 152 kJ were destroyed to generate 1 mol of hydrogen with that process configuration. By a
368 careful choice of temperature and S/C, energy and exergy efficiencies could reach values of *ca.*
369 85% and 75% respectively, with an optimized H_2 production of 4.89 moles of H_2 per mol of glycerol
370 at 900 K, S/C=1.8 and O/C=0.3. Since no experimental validation of these results was conducted,
371 these conclusions should be taken cautiously.
372 Following a similar approach to that by Authayanun *et al.* [56], Leal *et al.* [59] conducted a
373 thermodynamic study of the OSR of model CG using Aspen Plus, though introducing *in-situ* CO_2
374 and/or H_2 separation to produce high-purity hydrogen. *In-situ* separation of H_2 or CO_2 (*e.g.,*
375 through a perm-selective membrane) increased H_2 and CO_2 production in the OSR reactor, while
376 inhibiting the formation of CO and CH_4. The maximum hydrogen yield could be achieved at lower
377 temperatures in a membrane reformer, compared to a traditional reactor. As occurs with the work
378 by Hajjaji *et al.* [58], these conclusions were not validated against experimental data, and must
379 be considered with caution.
380 Because synthetic CG had not been properly modelled in previous thermodynamic studies,
381 Ibrahim's group conducted a thermodynamic analysis of the OSR process considering different
382 mixtures of synthetic CG [51], including different components typically found in CG such as
383 methanol, soap and oleic acid. HYSYS software was used to analyze the influence of the main
384 operating conditions on hydrogen yield. In spite the findings and conclusions from the study were
385 in line with previous studies, the presence of all three impurities lowered the equilibrium values of
386 H_2 and CO yields in comparison to those obtained for pure glycerol. When varying the usual
387 process parameters, similar trends to those obtained for pure glycerol were found in

thermodynamic equilibrium data. The main interest of this work lies on the thermodynamic data presented for synthetic CG compositions, which included the presence of different kinds of impurities.

4. State-of-the-art in the oxidative steam reforming of glycerol

The OSR studies can be divided into two main categories depending on the metallic active phase of the catalysts: transition non-noble metals (usually Ni is the selected active metal) and catalysts based on noble metals (Pd, Rh and Pt).

4.1. Transition non-noble metal-based catalysts (Ni, Co, Mn)

Table 2 compiles the most relevant studies on OSR of glycerol using transition metal catalysts.

400 Table 2 – Summary of the studies on the OSR of glycerol using transition metal catalysts (X_G=glycerol conversion, Y=yield, S=selectivity).

T (K)	Oxygen ratio	Steam ratio	Catalyst	WHSV (W/F_{A0})	GHSV	X_G (%)	H_2 (Y or S)	CO (Y or S)	H_2/CO	H_2 (content)	CO (content)	Ref.
823-1023	O/C=0.3	S/C=3	Ni-Pd-Cu/K-Al_2O_3	-	-	-	Y=3-58%	-		50-60%	-	[60]
1043-1083	O_2/C=0.4-0.7	S/C=2.0-2.7	Ni commercial (Süd Chemie G91 EW)	-	-		Y=1.3-3.5 mol/mol G	Y=0.5-1.2 mol/mol G		-	-	[61]
823-923	O_2/G=0.25-0.75	S/G=3-9	Ni/CeO_2-ZrO_2/Al_2O_3 and Ni/Al_2O_3	-	1.6×10^4 h^{-1}	45-99	Y=25.0-80.9%	Y=25.9-49.0%	-	-	-	[62]
773-973	O_2/G=0-0.3	S/G=3-9	Ni/CeO_2/Al_2O_3 catalyst and Pd/Ag membrane	5 h^{-1}	-	59.6-99.6	Y=19-85.3	S=23-80	-	-	-	[63]
923-1073	10% O_2, 20% H_2O, 20% $C_3H_8O_3$ in N_2 or 10% O_2, 40% H_2O, 10% $C_3H_8O_3$ in N_2	-	Ni-Ru/ $La_{0.8}Pr_{0.2}Mn_{0.2}Cr_{0.8}O_3/Y_{0.08}Zr_{0.92}O_{2-\delta}$/microchannel substrate and Ni-Ru/ $Sm_{0.15}Pr_{0.15}Ce_{0.35}$-$Zr_{0.35}O_2$/ microchannel substrate	-	-	-	S≃70%	S≃60%	-	14-26	12-26	[64]
873-1073	10.9% $C_3H_8O_3$, 9.5% O_2, 44.5% H_2O, 35.1% N_2 or 20% $C_3H_8O_3$, 20%	-	Ni-Ru/ $La_{0.8}Pr_{0.2}Mn_{0.2}Cr_{0.8}O_3/Y_{0.08}Zr_{0.92}O_{2-\delta}$, $LaNi_{0.95}Ru_{0.05}O$/Mg-Al_2O_3 and Ni-Ru/$MnCr_2O_4$/ microchannel substrates	-	-	45-100	S≃60%	S≃60%	-	6-25	5-26	[65]

	H_2O, 20% O_2, 20% N_2		(SiC/Al-Si-O, α-Al_2O_3/Al-Si-O, Ni-Al and Fechraloy plates)									
723-973	O/G=0.2-0.8	S/G=6-12	Ni/$Ce_{0.5}Zr_{0.33}M_{0.17}O_{2-\delta}$ (M = Mg, Ca, Y, La or Gd)	-	-	19-95	S=11-99	-	-	44-60	8-17	[66]
773-923	O/C=0.2-0.8	S/C=1.6-3.6	Ni/$Ce_{0.5}Zr_{0.33}M_{0.17}O_{2-\delta}$ (M = Mg, Ca or Gd)	-	-	53-95	S=43-88% or Y=0.58-1.42 mol/mol G	-	-	-	-	[67]
773-873	C/O=0.75-2.25	S/C=3-6	Ni/Al_2O_3/Fecralloy plate	2.9×10^5 ml/g_{cat}.h^{-1}	1×10^5 h^{-1}	2-72	Y=0.03-1.09 mol/mol G	Y=0.05-1.67 mol/mol G	-	-	-	[68]
823-1023	O/C=0.51	S/C=4	$CoAl_2O_4$ disperser in SiC, SiO_2 and γ-Al_2O_3	(3.5 g_{cat}·min/g G)	1.1×10^4 h^{-1}	83-94%	Y=11-90 mg/g G	Y=83-559 mg/g G	0.3-2.5	18-61	4-60	[69]
923	O_2/G=0.5	S/C=3.7	Ni-$La_2(Ce_{1-x}Zr_x)_2O_7$ (x=0, 0.5, 1)	3 h^{-1}	-	>99.7	Y=70-89%	-	-	59.7-60.3	2.8-3.1	[70]
882-1188 (adiabatic)	C/O=0.8-1.2	S/C=0-4/3	$LaMnO_3$ and $LaNiO_3$ perovskites	-	-	24.3-100	S=1.9-128.5%	S=2.5-62.7%	0.3-15.8	-	-	[71]

401

402

Swami and Abraham [60] studied the effect of temperature on char formation during isothermal SR and OSR of pure glycerol over a Ni-Pd-Cu/K-Al_2O_3 catalyst. The hydrogen yield by OSR was higher than by SR at all tested temperatures, except at 823 K. Moreover, the hydrogen yield in OSR increased always with the temperature, while in SR it almost leveled at temperatures ≥923 K. By increasing the oxygen feed, an increase in H_2 yield was found. The SR was surface-reaction controlled at lower temperatures (823-923 K) and was mass-transfer controlled at higher temperatures (973-1123 K), while the OSR was mass-transfer limited at all temperatures (except at 823 K). Therefore, feeding small amounts of oxygen at high S/C minimizes char formation, and allows to operate for longer periods.

A 2^3 factorial experimental design was used by Douette *et al.* [61] to study the reforming of both reagent grade and CG (glycerol content not specified) using a commercial Ni catalyst. The highest hydrogen yield (4.6 mol $H_2 \cdot mol^{-1}$ glycerin) was obtained by SR (without oxygen feed) at S/C=2.2, and a reformer internal temperature of 1077 K [61]. Such yield corresponded to 65% of the stoichiometric maximum and 85% of the theoretical maximum based on chemical equilibrium. The O/C ratio had the greatest effect over the range of tested conditions. Next, a secondary WGS reactor operating at 642 K was coupled downstream of the reformer, and the hydrogen yield increased (to 5.3 mol $H_2 \cdot mol^{-1}$ glycerin). With CG, the initial results were very close to those achieved with reagent-grade glycerin, but upon time-on-stream the hydrogen yield decreased due to catalyst deactivation, coking and deposits formation in the reformer. Tests conducted with reagent-grade glycerin doped with potential contaminants (methanol, NaOH, and NaCl) indicated that Na was one of the elements responsible for catalysts' activity loss.

Kamonsuangkasem *et al.* [62] studied the OSR of yellow glycerol (a product of CG purification, with a 94 wt.% of glycerol) over a Ni/CeO_2-ZrO_2/Al_2O_3 catalyst. Nearly complete conversion of glycerol, a hydrogen selectivity of 69% and a yield of 67% were achieved at 923 K, S/G=9 and O_2/G=0.5. By increasing the reaction temperature and the S/G, both glycerol decomposition and SR were enhanced, resulting in higher conversion, as well higher yields and selectivities to H_2 and other gas products. In contrast, by increasing the O_2/G the glycerol conversion was generally improved but H_2 selectivity significantly decreased due to the oxidation of hydrogen. More CO than CO_2 was generated in the oxygen-rich environment, and more carbon was formed on the catalyst by hydrogenation of the CO.

Lin *et al.* [63] studied the production of hydrogen by OSR of glycerol in a packed-bed reactor over a Ni/CeO_2/Al_2O_3 catalyst and Pd/Ag membrane reactor [63,72]. In the packed-bed reactor, a glycerol conversion of 99.6% was achieved; however, the best hydrogen yield was 85.3% at 773 K, S/G=9 and O_2/G=0.15 [63]. The excess water caused the decline in glycerol conversion because it facilitates CO_2 formation by WGS, which then suppressed glycerol oxidation. In the Pd/Ag membrane reactor under the same operating conditions, the glycerol conversion increased with increasing pressure, but the CO selectivity and hydrogen yield decreased, which was attributed to methanation and reverse methane dry reforming reactions. The maximum glycerol conversion observed in the membrane reactor was 51.7%.

Sadykov *et al.* [64] studied the OSR of glycerin over two types of nanocomposite active components (Ni-Ru/$La_{0.8}Pr_{0.2}Mn_{0.2}Cr_{0.8}O_3$/$Y_{0.08}Zr_{0.92}O_{2-\delta}$, and Ni-Ru/$Sm_{0.15}Pr_{0.15}Ce_{0.35}$-$Zr_{0.35}O_2$) supported on microchannel substrates. Both catalysts yielded stable operation for 30 h with reasonably high syngas yields, and oxygen addition to the feed allowed to suppress coking, but liquid byproducts and ethylene were also produced. Decreasing glycerol content in the feed caused an increase in CO_2 selectivity and a decrease in CO selectivity, possibly caused by the WGS reaction. The efficiency of the developed catalysts was demonstrated because glycerol conversion into syngas and methane with some traces of ethane was complete at 973 K.

In a related study, Sadykov *et al.* [65] worked on the OSR of glycerol over three nanocomposite active components (Ni-Ru/$La_{0.8}Pr_{0.2}Mn_{0.2}Cr_{0.8}O_3$/$Y_{0.08}Zr_{0.92}O_{2-\delta}$, $LaNi_{0.95}Ru_{0.05}O$/Mg-Al_2O_3 and Ni-Ru/$MnCr_2O_4$) supported on three microchannel substrates. The conversion consistently increased with temperature over the Ni-Ru/$MnCr_2O_4$ catalyst, being complete in the temperature range of 1023-1073 K. The concentrations of H_2 and CO_2 increased while those of CO, CH_4 and C_2 hydrocarbons decreased as the temperature increased, an effect attributed to reforming and WGS reactions. Stable performance was observed over the Ni-Ru/$La_{0.8}Pr_{0.2}Mn_{0.2}$-$Cr_{0.8}O_3$/$Y_{0.08}Zr_{0.92}O_{2-\delta}$ catalyst for 20 h of steady operation, even with a higher glycerol content and a lower steam content in the feed while keeping the O/C constant. The authors anticipated that further optimization of microchannel configuration as well as C/O and S/C may allow to achieve the complete conversion of glycerol along with higher syngas yield.

Sabri *et al.* [66] studied the OSR of glycerin over Ni catalysts supported on $Ce_{0.5}Zr_{0.33}M_{0.17}O_{2-\delta}$ (M = Mg, Ca, Y, La or Gd). They investigated the role of the metal promoters on the physicochemical

properties of the catalyst and the catalytic activity. Among the tested catalysts, Ni/CeZrGd presented a low coke formation rate (47.3 $mg \cdot g^{-1} \cdot h^{-1}$ at 773 K, S/G=6 and O/G=0.5), high surface area and pore volume, and the best performance at all tested reaction temperatures. For such reason, a parametric study was performed with this catalyst. The catalyst performed better in OSR of glycerol than in SR in terms of conversion and H_2 selectivity. The conversion and H_2 selectivity increased (up to 82 mol.% and 70 mol.%, respectively) rapidly with the increase in temperature until 873 K.

To investigate the effects of impurities and promoters (Gd, Mg and Ca), the same research group continued the study on the OSR over Ni catalysts supported on cerium-zirconium, this time using a synthetic CG (45.6 wt.% glycerol) [67]. The addition of methanol and soap to pure glycerol caused a decrease in the performance of the Ni/CeZrGd catalyst during OSR, which was attributed to the formation of carbonaceous deposits over the catalyst. However, the addition of ash (with KCl and NaCl) allowed to recover the catalytic activity, which was attributed to their positive effect on the oxidation of carbon deposits on the catalyst surface. Slight increases in conversion and H_2 yield were observed upon the addition of oleic acid, but no significant effects were observed on the activity of the Ni/CeZrGd catalyst. Ni/CeZrCa showed the best performance in the OSR of the synthetic CG, which was ascribed to the reducibility, nickel dispersion, low coke deposition (nearly zero at 873 K, S/C=2.6 and O/C=0.8), pore volume and surface area properties. For such reasons, the authors performed a parametric evaluation using this catalyst. At O/C=0.20, hydrogen selectivity increased with an increase in S/C, but conversion decreased. The hydrogen selectivity, TOF and synthetic CG conversion increased with an increase in the reaction temperature, however, such increases were overturned by considerable amounts of carbon deposits at reaction temperatures $\leq$823 K. Therefore, suitable operating conditions were found to be 823 K, S/C=2.6 and O/C=0.5. A statistical analysis revealed that reaction temperature is the most influential parameter on the conversion of synthetic CG, followed by O/C, S/C, and calcination temperature. The S/C and O/C were the most influential in terms of hydrogen selectivity, whilst O/C and calcination temperature were the most effective based on TOF.

Moreira *et al.* [69] worked on the OSR using a $CoAl_2O_4$ spinel coprecipitated catalyst to produce syngas from glycerin. Different bed fillers (SiC, SiO_2 and γ-Al_2O_3) were studied, as well as the catalyst reuse. Using a bed of commercial γ-Al_2O_3, around 90% of the carbon fed into the reactor

493 was converted to gaseous products, yielding a syngas with $H_2/CO \simeq 1$ [69]. In the catalytic
494 experiments, the highest hydrogen production was attained using silica as bed filler, followed by
495 alumina and silicon carbide. The carbon conversion to gas increased slightly with temperature,
496 and the highest hydrogen production was achieved at 823 K with no observable catalyst
497 deactivation upon 4 h of reaction. The catalyst structure changed drastically after reaction in
498 comparison to the fresh or the regenerated catalyst. A single run using the Co/Al-spinel catalyst
499 resulted in coke encapsulation covering of the catalyst particles, which had a very clearly defined
500 hexagonal shape conformed over the surface of the catalyst particles. Upon four reuse and
501 regeneration cycles, the catalyst could effectively maintain its activity for a combined total time-
502 on-stream of 20 h at 1023 K. Upon the regeneration of the catalyst by oxidation, Co-rich species
503 migrated from the core of the deactivated particles to the surface and became partially
504 agglomerated. The core-shell structures were completely transformed, and Co species migrated
505 to the surface over the Co spinel structure, thus acting like a Co reservoir, which could explain
506 the complete recovery of activity once the catalysts were subsequently activated before the next
507 reforming reaction cycle.
508 Veiga *et al.* [70] investigated the reforming of industrial CG (64 wt.% glycerol) over catalysts
509 having the general formula: Ni-$La_2(Ce_{1-x}Zr_x)_2O_7$ (x=0, 0.5, 1). They studied the SR and OSR of
510 CG, and the substitution of zirconium by cerium cations (x=0.5). The H_2 yield was much higher in
511 OSR than in SR experiments. C_2-C_3 hydrocarbons were almost absent in OSR experiments, while
512 in SR a low production was observed. In both reforming processes, analyses of condensates
513 revealed the presence of different intermediates, such as acetaldehyde, methanol, ethanol,
514 acetone, acetic acid, ethane-1,2-diol, and propane-1,2-diol. Globally, catalysts having Zr
515 performed slightly better in terms of stability than those without it, while those containing both Ce
516 and Zr performed even better especially in SR tests. The highest stability was observed in
517 experiments with NiLaCeZr catalyst, which was attributed to more efficient carbon removal from
518 the boundaries of active site due to the highest basicity. The higher basicity implies that there are
519 more oxygen vacancies with higher mobility, which helped in the stabilization of the catalyst
520 particles against sintering and coking, while acidity was reported to promote dehydrations
521 reactions of oxygenates to olefins which are known coking precursors. The origin of carbon
522 deposits was investigated in both processes by temperature programmed oxidation (TPO). The

523 carbon deposits on the catalyst used in OSR were burned at low temperatures (623-723 K),
524 indicating their amorphous and encapsulating nature as well as their ease of removal. After their
525 use in SR, the catalysts presented more structured deposits (filamentous and graphitic), which
526 are more difficult to remove. The reuse of the NiLaCeZr catalyst in OSR was addressed. A
527 decrease in H_2 yield (from 89% to 70%) was observed in the first utilization of the fresh catalyst
528 for 20 h on stream. After catalyst regeneration (with an O_2/Ar mixture), the H_2 yield was partially
529 recovered (79%) but the carbon removal was not enough to completely regenerate the active
530 sites. However, after the second regeneration, the initial H_2 yield was almost completely
531 recovered (85%), thus showing an efficient removal of alkali present in CG.
532 The use of La perovskites with Ni or Mn was explored by Liu and Lin [71] in the OSR of glycerol,
533 by preparing impregnated cordierite monoliths with the active-phase deposition method. $LaMnO_3$
534 monoliths were more active and stable than $LaNiO_3$, though they promoted combustion over
535 partial oxidation to syngas, whilst the latter were more selective to syngas but much less stable
536 than their Mn counterparts. Surface welding, cracking, and loss of the perovskite active phase
537 due to segregation and/or transformations into other phases (such as La_2NiO_4) were signaled as
538 the main causes for the loss of activity in the stability tests carried out over 24 h.
539

540 **4.2. Noble metal-based catalysts**

541 Table 3 compiles the most relevant studies on OSR of glycerol using noble metal catalysts. All
542 the OSR studies reported so far with noble metal catalysts attempted process intensification
543 through the development of structured catalytic reactors, mainly by using monoliths over which
544 the active phase was deposited. Process intensification will be discussed more in depth later in
545 section 4.4.
546

547 Table 3 – Summary of the studies on tOSR of glycerol using noble metal catalysts (X_G=glycerol conversion, Y=yield, S=selectivity).

T (K)	Oxygen ratio	Steam ratio	Catalyst	WHSV (W/F_{A0})	GHSV	X_G (%)	H_2 (Y or S)	CO (Y or S)	H_2/CO	H_2 (content)	CO (content)	Ref.
873-1473 (adiabatic)	C/O=0.6-1.8	S/C=0-4.5	$RhCeAl_2O_3WC$-monolith	-	10^5 h^{-1}	>99	S=43-79%	S=25-50%	0.9-3.9	-	-	[73]
573-1273 (adiabatic)	C/O=1.4-2.0	S/C=0-5/3	$RhCeAl_2O_3WC$/monolith and Pt/monolith	-	-	70-100	S=25-90%	S=25-60%	1.1-3.9	-	-	[45]
1023-1323	C/O=0.8	S/C=2/4	Rh-Ce/CeO_2/Al_2O_3	-	10^6 h^{-1}		S=20-60%	S=38-58%	0.5-2.0	-	-	[46]
923	C/O=1	S/C=2	Ir/La_2O_2	-	10^4 h^{-1}		S=60%	S=20%		-	-	[57]
1036-1428 (adiabatic)	C/O=0.8-1.2	S/C=0-4/3	Pt-$LaMnO_3$/cordite monolith, $LaMnO_3$/cordite monolith, Pt/cordite monolith	-	-	40-100	S=30-122%	S=9-63%	0.9-10.7	-	-	[74]
882-1188 (adiabatic)	C/O=0.8-1.2	S/C=0-4/3	$LaMnO_3$ and $LaNiO_3$ perovskites	-	-	24.3-100	S=1.9-128.5%	S=2.5-62.7%	0.3-15.8	-	-	[71]
573-973	O_2/C=0.1-0.3	S/C=0.4-1.5	Pt/cordite monolith and Pt-Rh/cordite monolith	-	-	45-98	Y=26-88%	Y=59-70%	0.75-1.9	18-55	22-71	[47]
823-973	O_2/C=0.1-0.7	S/C=1-3	Pt/cordite monolith and Pt-Rh/cordite monolith	-	5×10^3-2.3×10^4 h^{-1}	80-98	S=24-85%	S=18-60%	-	50-58	26-29	[49]
823-973	C/O=0.75-1.125	S/C=3-5	Rh/Al_2O_3/Fecralloy plate	4.8×10^3 $ml/g_{cat}\cdot min^{-1}$	-	93-100	Y=0.2-2.2 mol/mol G	Y=1.2-2.1 mol/mol G	0.2-1.5	-	-	[75]

548

549

550 Dauenhauer *et al.* [73] worked on the catalytic PO and OSR of glycerol using a Rh and Ce catalyst
551 supported on a ceramic monolith of α-Al_2O_3/SiO_2 coated with γ-Al_2O_3. By adding steam to the gas
552 feed, the temperature decreased to *ca.* 573 K with no effects on glycerol conversion (100%), and
553 no significant carbon deposition over the catalysts was observed. During PO experiments, H_2
554 selectivity was close to equilibrium for C/O<1.2 and became lower for C/O>1.3, while CO
555 selectivity was always above the equilibrium for all tested conditions. In OSR experiments, H_2
556 selectivity increased and approached equilibrium at increasing C/O≤0.9, and then decreased and
557 strongly departed from equilibrium for C/O>1.0. At the same time, CO selectivity showed a
558 complementary behavior by decreasing and approaching equilibrium at increasing C/O ratios up
559 to 0.9, then increasing and departing from equilibrium for C/O>1.0. The remaining carbon from
560 reactant glycerin was reformed to CO_2 and the minor products (methane, acetaldehyde, ethane,
561 and ethylene). The surface reactions appear to dominate for the conditions used in the
562 experiments, meaning that adsorption of hydroxyl groups of glycerol bonded on noble metal
563 surfaces as alkoxide species that completely decompose into H_2 and C_1 products.
564 In a follow-up work, with the purpose of generating syngas for the production of methanol, while
565 improving the sustainability of the biodiesel production in a circular economy perspective, PO and
566 OSR of glycerol were studied over Rh-Ce and Pt catalysts supported on a ceramic monolith of α-
567 Al_2O_3/SiO_2 [45]. Over Rh-Ce catalysts, most of the products approached the equilibrium
568 selectivities in PO experiments, while in OSR the addition of water caused a decrease in
569 temperature resulting in the departure of selectivities from equilibrium, in agreement with their
570 previous study. In the case of Rh-Ce, liquid water can be added to glycerin up to S/C=2/3 to
571 increase H_2 production. A variety of H_2/CO ratios were observed by adjusting the C/O and S/C,
572 while large amounts of non-equilibrium chemicals were detected for C/O≥1.4 in the case of Pt
573 catalyst. Acrolein, acetaldehyde, and hydroxyacetone were major condensable products resulting
574 from the pyrolysis of glycerol, while methylglyoxal was produced heterogeneously. Interestingly,
575 the authors estimated that *ca.* 40% of the methanol demand in a biodiesel plant could be satisfied
576 by converting glycerol into syngas without the addition of any process heat, and anticipated that
577 higher yields may be possible in industrial-size units.

Rennard *et al.* [46] continued the study for obtaining syngas from glycerin for methanol production. As in previous works [45,73], a Rh-Ce catalyst was used, taking advantage of its high stability and its enhancements in dispersion caused by Ce addition, sintering reduction and oxygen transfer. Two aging studies were performed to examine the stability of a Rh-Ce/CeO_2/Al_2O_3 catalyst. The catalysts were subjected to two different types of tests in a fixed-bed quartz reactor: (1) an accelerated aging study for 353 h on stream subjecting the catalyst to extremes in temperature and chemical environment to simulate transient processes, and (2) a steady state aging study for 450 h on stream without any externally triggered events while maintaining the reactor at temperatures <1323 K. Catalyst deactivation was perceived by the change in gas composition (decrease in H_2 and CO_2 and increase in CO selectivities). The changes in the produced gas composition suggested inhibition in the WGS reaction, which is typically promoted by Ce. Scanning electron microscopy (SEM) indicated sintering of the catalyst due to high reaction temperatures, while energy-dispersive X-ray spectroscopy (EDS) showed inorganic deposits on the walls of the quartz reactor and on the catalyst spheres.

Yang *et al.* [57] complemented their parametric thermodynamic study (see discussion on this study above) with experiments of catalytic OSR of glycerol and ethanol over an Ir/La_2O_2 catalyst, and observed that hydrogen selectivity was below the equilibrium predictions. Higher C/O and S/C ratios favored H_2 production., The reaction temperature should be in the 873-1023 K range due to the limitation of WGS reaction, and the C/O should be in the 0.8-1.2 range to maximize the hydrogen yield under OSR conditions.

In a follow-up of the work conducted using transition metal-based perovskites with Ni or Mn, Liu and Lin [76] prepared single Pt-, $LaMnO_3$-, and Pt/$LaMnO_3$-coated cordierite monoliths and tested them in the OSR of glycerol. Significant sintering was observed in the case of the Pt-coated monolith. Some cracks and welding appeared after 28 h of testing in the case of the Pt/$LaMnO_3$-coated monolith, though Pt thermal sintering could be avoided. $LaMnO_3$ and Pt/$LaMnO_3$ were more active than the Pt catalyst. No carbon deposits were observed in any case, and Pt supported on $LaMnO_3$ was deemed the optimal catalyst design. Pt activates water for reforming and the WGS reaction to enhance H_2 selectivity while $LaMnO_3$ reduces unwanted byproducts, stabilizes Pt clusters, and aids autothermal reactions in steam-rich conditions.

607 Recently, Avci's group has studied the oxidative steam reforming (OSR) of glycerol to syngas in
608 a microchannel reactor composed of a Rh/Al_2O_3 catalytic layer coated on the inner wall of a
609 Fecralloy rectangular channel [75]. Complete coke-free conversion of glycerol to gaseous carbon
610 containing species at most of the tested operating conditions was achieved. Only at 823 K and
611 C/O = 1.125 carbon deposition was significant despite having 93% glycerol conversion. Under
612 identical conditions, an uncoated microchannel reactor packed with the Rh/Al_2O_3 catalyst in
613 powder form performed worse in the OSR of glycerol, yielding less CO_2 and H_2 and increasing
614 the yields of CO and C1-C2 hydrocarbons.
615
616 **4.3. Critical discussion on the development of catalysts for the oxidative steam reforming**
617 **of glycerol.**
618 From the discussion above it can be concluded that more in-depth studies on the deactivation of
619 catalysts, and on the optimization of the catalyst formulations are needed in the OSR of glycerol.
620 Regarding transition non-noble metal-based catalysts, most of the studies rely on previous
621 existing knowledge on the development of active catalysts for the non-oxidative SR of glycerol
622 and ethanol. In the case of Ni-based catalysts, severe deactivation by coking is still an issue that
623 needs to be addressed in the OSR of glycerol. As evidenced by Kamonsuangkasem *et al.* [62],
624 filamentous and graphitic carbon could be found in the OSR of pure and yellow glycerol despite
625 using relatively high S/C and O/C ratios (9 and 0.5 respectively). Rapid decays in activity have
626 been observed in long activity tests or in studies conducted at high space velocities. In addition,
627 the loss of active phase, caused by reoxidation of transition metal-based particles or by its
628 transformation into other less active species, has not been systematically addressed yet. Sintering
629 of the active phase is another cause for the loss of active phase leading to catalyst deactivation.
630 In glycerol reforming the sintering phenomenon is intensified by the use of high S/C ratios [68]
631 and high reaction temperatures [46]. In consequence, the development of stable catalysts that
632 can sustain their performance over long periods of time is still pending.
633 As for noble metal-based catalysts, the most promising results have been found for Rh as active
634 phase, though more fundamental studies on the actual role displayed by the different catalytic
635 formulations are missing. The studies that selected noble metals for the OSR of glycerol focused
636 on the use of structured catalytic reactors, mostly in the form of wash-coated monoliths, in which

637 a catalytic layer containing the noble metal active phase was deposited. However, prior to the
638 structuring process, it is necessary to gain deeper insight on the reaction mechanisms and overall
639 performance of the catalyst formulations in powder form. Optimization of the noble metal content
640 in the formulations is still pending. Schmidt's group lowered the noble metal loading to 1.2 wt.%
641 [46], though this is still insufficient for scaling-up the catalytic reactor and make the technology
642 economically viable.
643 Furthermore, the effect on catalyst deactivation of certain impurities typically found in CG, such
644 as S-containing species, which could cause rapid activity loss by poisoning, has not been
645 analyzed in depth either. Other impurities including Na and K salts often present in CG have been
646 reported to cause a significant decay in activity in the OSR [61], and could have some impact on
647 the formation of deposits and possibly lead to pressure build-up and clogging problems. However,
648 other authors reported a beneficial effect of the addition of KCl and NaCl on the recovery of the
649 catalytic activity [67]. Therefore, further studies using CG as feedstock should be developed to
650 assess the performance of glycerol OSR catalysts in the presence of salts, and to clearly elucidate
651 their role on their syngas activity and long-term stability. Most of the literature that analyzed the
652 effect of CG impurities focused on the effect of methanol, soap or free fatty acids derived from
653 the biodiesel production process on the catalytic performance. In general, these impurities caused
654 a significant decay in the activity of transition non-noble metal-based catalysts by carbon
655 deposition.
656 Those studies that sought to develop stable catalysts for glycerol OSR aimed at the enhancement
657 of the metallic dispersion and the stabilization of the active phase, by using modifiers of the active
658 phase and/or the support, often leading to very complex formulations. However, new proofs-of-
659 concept should be considered prior to further developing new sophisticated but probably non-
660 viable catalysts. As demonstrated by Ayoobi and Shoegl [77], complete conversion of glycerol
661 OSR can be effectively attained for producing quality syngas without the need of a catalyst at
662 temperatures around 1173 K. In fact, in our previous work [69], it was evidenced that around 90%
663 of the glycerol fed into the OSR reactor can be effectively converted to product gas without the
664 need of a catalyst, just by thermal decomposition on bulk inexpensive bed fillers such as silica or
665 alumina at temperatures as low as 1073 K. Bearing this in mind, most of the carbon deposits can
666 thus be avoided while preventing the deactivation of catalysts by coking. This in turn could impact

667 on the catalyst design, which should be oriented toward new formulations with high selectivity for
668 syngas and capable of tuning the product gas composition downstream from the glycerol
669 decomposition zone inside the reactor.

670

671 **4.4. Intensification of the OSR of glycerol by means of structured catalytic reactors and**
672 **microreactors**

673 Structured catalytic reactors can contribute to facilitate the viability of scaling-up the catalytic OSR
674 of glycerol, owing to their superior performance over other catalytic reactors such as packed-bed
675 reactors. They allow an easier thermal integration, higher energy efficiency, high rates of heat
676 and mass transfer, and reduced mixing times. These advantages permit to exploit the full potential
677 of very active catalysts and to achieve high production capacity in compact units. In this section,
678 the state-of-the-art on the intensification of the OSR of glycerol by developing structured catalytic
679 reactors and microreactors is discussed.

680 Liu *et al.* [47] contributed to the process intensification of glycerol OSR using structured catalytic
681 reactors and a BASF dual layer monolith catalyst. The catalyst consisted of a cordierite monolith
682 wash-coated with 1-4 wt.% of precious metals (Pt and Rh/Pt) on a zirconia-based support. The
683 novel concept of the dual catalytic layer resides in its design and structure, which allow for an
684 integrated and more efficient heat management. By having a dual layer of only 5-10 μm thickness
685 each, mass and heat transfer limitations are minimized. The outer layer catalyzes the exothermic
686 PO reaction, whilst the inner layer catalyzes the endothermal SR reaction. The heat produced by
687 PO is thus effectively absorbed by the adjacent catalytic layer and drives the SR reaction. Liu *et*
688 *al.* [47] studied the effects of the distance between the feed atomization nozzle and the catalyst
689 ($\simeq$0.5-7.6 cm), temperature, S/C and O_2/C on product composition and performance in catalytic
690 and non-catalytic conditions. The optimum distance between the nozzle and the catalyst was
691 $\simeq$5.1 cm, and the catalyst had no effect on the glycerol conversion at temperatures up to 773 K,
692 but dramatically changed the product composition at all tested temperatures by promoting the SR
693 and WGS reactions. Moreover, the optimum operating conditions were O_2/C=0.15, S/C=0.8 and
694 T=923 K which allowed to achieve high glycerol conversion (95%), high H_2 yields (ca. 58%) and
695 H_2/CO$\simeq$2 with minimal coke formation upon 30 h on stream.

696 Continuing that work, Liu and Lawal [49] performed an thermodynamic analysis and
697 characterization of syngas production by OSR of biodiesel byproducts. A BASF dual layer wash-
698 coated monolithic catalyst was used, consisting of Pt in the catalytic PO layer and Rh/Pt in the
699 SR layer, this time on a γ-alumina support. They achieved a total gaseous carbon yield of 98%
700 with near-equilibrium concentrations of H_2, CO, CO_2 and CH_4. The optimum operating conditions
701 to produce high yields of syngas with minimal coke formation were found at 1023 K, S/C=3, and
702 O_2/C=0.1. The rapid increase in the yields of H_2 and CO with the increase in reaction temperature
703 was attributed to endothermic decomposition and SR of both methanol and glycerol. CO_2 was
704 primarily produced by the catalytic PO reaction, which was thermodynamically favored by low
705 temperature, and S/C≥1 should be used to diminish coke formation.
706 In a follow-up work, Liu and Lawal [48] studied the kinetics of glycerol OSR using the same
707 catalyst employed in their previous publication [49]. A more detailed discussion on the kinetic
708 study can be found in section 5 (see below). The reaction rate of glycerol reforming was not limited
709 by mass transfer within the wash-coated catalyst layers; the apparent heat of reaction was close
710 to zero because the heat produced by PO reaction was consumed instantly by SR and the radial
711 heat transfer limitation could be neglected.
712 The use of noble metals as catalytic active phases in structured catalytic reactors has also been
713 explored in the OSR of glycerol. Liu and Lin [74] studied the autothermal PO of glycerin over Pt,
714 $LaMnO_3$ and Pt/$LaMnO_3$ supported on cordierite honeycomb monoliths coated with γ-alumina.
715 Despite sintering seriously damaged the catalyst at high temperatures, the highest H_2 production
716 was observed over the Pt catalyst, attributed to its activity in reforming and WGS reactions. Bare
717 $LaMnO_3$ perovskite favored combustion, generating heat for autothermal operations. A glycerol
718 conversion of 98% and a H_2/CO=2.1 were achieved under optimized operating conditions
719 (S/C=2/3 and C/O=1.1) over the Pt/$LaMnO_3$ catalyst. Pt/$LaMnO_3$ was the best catalyst because
720 Pt activates water for reforming and WGS reactions, while $LaMnO_3$ diminishes byproducts,
721 stabilizes Pt clusters, and assists autothermal reactions.
722 To overcome the sintering problems observed in their previous work [74] while taking advantage
723 of the stability and oxidation activity of $LaMnO_3$, Liu and Lin [71] proceeded their study on glycerol
724 OSR by comparing the performances of $LaMnO_3$ and $LaNiO_3$ perovskites supported on cordierite
725 monoliths. $LaMnO_3$ favored glycerol combustion (in accordance with their previous study),

726 generating more CO_2, H_2O, and heat to sustain autothermal operation. Conversely, $LaNiO_3$
727 promoted glycerol PO to syngas, producing more H_2 and CO but generating less heat and being
728 unable to sustain autothermal operation in steam-richer environments. However, $LaNiO_3$ was
729 more active in SR and WGS, leading to higher H_2 production. The highest H_2 selectivities for both
730 for $LaMnO_3$ and for $LaNiO_3$ perovskites were observed at S/C=1/3 and C/O=1.1. Increasing S/C
731 or C/O led to lower the reaction temperature and glycerol conversion. Despite that welding and
732 cracking were observed on both perovskites after 24 h on stream, $LaMnO_3$ was more stable than
733 $LaNiO_3$ in autothermal PO.
734 More recently, Koc and Avci [68] studied the SR and OSR of glycerol in a microchannel reactor
735 coated with Ni/Al_2O_3 over a Fecralloy plate. In SR, glycerol conversion and yields of H_2, CO, CO_2,
736 CH_4, C_2H_4 and C_2H_6 generally increased with the increase in temperature. The increase in S/C
737 promoted the gasification of carbon deposits, the WGS activity and improved the yield of H_2. The
738 increase in Ni load (from 5% to 10%) did not correspond to an equivalent improvement in
739 conversion and product yields, an effect attributed to Ni sintering. Moreover, the conversion
740 decreased upon the increase in feed rate but improved the H_2/CO and CO_2/CO ratios, an effect
741 attributed to the decrease in the extent of glycerol decomposition and to the increase of WGS
742 activity. In OSR, carbon deposition decreased with the increase in S/C and O/C, and the addition
743 of oxygen improved glycerol conversion and product yields in comparison with SR results.
744 However, the glycerol conversion in OSR decreased with the increase in C/O (from 0.75 to 2.25)
745 as did the yield to CO_2, but the H_2 yield increased, and no particular trend was found for CO. OSR
746 blank experiments gave product yields comparable with those of the catalytic tests for CO and
747 CO_2. Moreover, glycerol conversions obtained in blank experiments (58.9-75.8%) carried out at
748 773-873 K were in fact slightly higher than those of catalytic experiments (58.4-71.7%).
749 Regardless of the operating conditions, the main role exerted by the catalysts was to shift the
750 product distribution in favor of H_2 and the reduction in the concentration of C_1-C_2 hydrocarbons.
751 Using a Rh/Al_2O_3 catalyst, the same research group conducted the study of OSR of glycerol in
752 two different reactor configurations: a packed-bed reactor and a coated microchannel reactor [58].
753 Rh remained in the reduced state, yielding no carbon deposition and complete consumption of
754 glycerol at all tested operating conditions, except at 823 K, C/O=1.125 and S/C=5, which was
755 attributed to coking. Regardless of the reaction temperature, the yield of CO_2 increased whereas

those of H_2, CH_4, C_2H_4, C_2H_6 and carbon deposition on the catalyst surface decreased when the C/O was reduced from 1.125 to 0.75. The changes in product yields with the temperature followed patterns that somewhat depended on the C/O ratio. Under the same operating conditions, the yields of H_2 and CO_2 obtained in the coated microchannel configuration were notably higher than those measured for the packed-bed configuration, an effect attributed to the improved heat transfer rates characteristic of coated microchannel reactors. In the presence of the catalyst the yields of H_2 and CO_2 were higher but that of CO was lower than in the absence of the catalyst, mainly attributed to the activity of the Rh/Al_2O_3 catalyst in the WGS reaction. The promotion of WGS reaction was confirmed by reducing S/C from 5 to 3, which led to decreasing yields of H_2 and CO_2, and increasing yields of CO. The concentrations of CH_4, C_2H_4 and C_2H_6 in the product gas were reduced by increasing temperature and decreasing S/C and C/O, an effect attributed to their consumption via oxidation and SR reactions. The catalyst did not affect conversion but changed the product distribution in favor of H_2. Finally, a syngas with H_2/CO=0.9-1.2 could be obtained in the coated microchannel reactor at T=973 K, S/C=3-4 and C/O=1.125, which were considered the best operating conditions.

5. Kinetics of oxidative steam reforming of glycerin

Kinetic studies are useful for understanding reaction mechanisms, thereby for optimizing processes and for optimized catalyst and chemical reactor designs. Presently, the literature on kinetic modelling of OSR of glycerol is scarce. The studies published by Lawal's and Ibrahim's research groups are the only known works that have dealt with kinetic modeling of OSR of glycerol to date. Ibrahim's group has studied the kinetics of hydrogen production by OSR of synthetic CG (45.6 wt.% glycerol) [78,79]. Synthetic CG composition was established by the analyses of the composition of CG samples from a major Canadian biodiesel producer. An empirical formula of $C_{2.5}H_7O_2$ was used to represent the overall reforming reactions of the synthetic CG. In Ghani *et al.* [78], a simple power rate law was proposed for modeling the kinetics of the catalytic OSR process using Ni/CeZrCa catalyst pellets in a packed-bed configuration. An integral analysis of the kinetic data obtained in 25 experimental runs was developed and estimation of the kinetic parameters was conducted using a modified genetic algorithm based on a fourth-order Runge-Kutta method. The varied operating conditions were the S/C, the O/C, the reaction temperature,

and the W/F_{A0}. The following equation was obtained, which reasonably predicted conversion data when compared to their empirical values (Eq. 21).

$$-r_A = k_0 e^{\left(-\frac{E_A}{RT}\right)} \cdot P_A^1 \cdot P_{H2O}^{0.5} \cdot P_{O2}^2 \quad \text{(Eq.21)}$$

Where A denotes CG, k_0 is the Arrhenius-type pre-exponential factor and E_a is the apparent activation energy. The following kinetic parameters were found: $k_0=2.09\cdot10^{11}$ mol $C\cdot g_{cat}^{-1}\cdot min^{-1}\cdot atm^{-3.5}$ and $E_a=93.7$ kJ·mol^{-1}. Equation 13 was proposed to be valid at atmospheric pressure for $773\geq T\geq923$ K, $1.6\geq S/C\geq3.6$, $0.05\geq O/C\geq=0.2$ and $0\geq W/F_{A0}\geq158$ $g_{cat}\cdot min\cdot mol^{-1}$ C. A similar expression was proposed in the kinetic study of OSR of purified glycerol (glycerol content not specified) using a $Ni/Ce_{0.5}Zr_{0.33}Gd_{0.16}O_{2-d}$ catalyst [80], though in this case the model had reaction orders 0.16, 0.74 and 0.49 with respect to glycerol, oxygen and steam (respectively) and an $E_a=53.3$ kJ·mol^{-1}.

In a subsequent study [79], the simulation of the catalytic reactor performance was done by developing a 2D pseudo-homogeneous numerical model using COMSOL Multiphysics software. The mass and energy conservation balances together with appropriate boundary conditions were numerically solved. The kinetics of the reaction was modelled using the expression above and the thermodynamics and chemical equilibrium were modelled using a Peng-Robinson Sryjek-Vera (PRSV) package developed in a previous study [51]. Despite power law rate models provide valuable insight on the kinetics of catalyzed reactions owing to their simplicity, their application is limited, since these models can only be applied when using similar operating conditions and types of catalysts.

In contrast, the development of mechanistic models such as Eley-Rideal (ER) types I and II or Langmuir-Hinshelwood-Hougen-Watson (LHHW) allow to gain deeper understanding of the whole process, thus improving the efficiency of designing and controlling tasks. However, to develop such type of models and provide expressions that can accurately predict reactants conversion is often complicated, especially in those cases where the global reaction set may be comprised of many different reactions as occurs in the case of crude hydrocarbon reforming [78]. Nevertheless, some authors have considered LHHW mechanistic models in the OSR of pure glycerol, which counts on a much more simplified global reaction set.

Liu and Lawal [48] tested several Langmuir-Hinshelwood (LH) type rate expressions for modeling the OSR of glycerol using a commercial structured catalyst supplied by BASF [81]. A more detailed discussion on this catalyst can be found above. In this kinetic study, an "atomic matrix" was presented, accounting for the only three atomic elements, namely C, H and O, constituting all possible reactants and products of the overall OSR reaction set, having a total of 6 different components: $C_3H_8O_3$, H_2O, O_2, CO, CO_2 and H_2 [48]. Based on that matrix, it was established that only 3 independent chemical reactions were needed: glycerol SR (Eq. 4), the WGS reaction (Eq. 3) and glycerol oxidation to CO (Eq. 22).

$$C_3H_8O_3 + 2\ O_2 \rightarrow 3\ CO + 4\ H_2O \qquad \text{(Eq.22)}$$

Both single- and dual-site LH mechanisms were considered for glycerol SR, as well as non-dissociative and dissociative glycerol adsorption on the alumina-supported catalyst. The net consumption rate of glycerol was assumed to be equal to the disappearance rate of glycerol in the SR reaction. The kinetic parameters were calculated by nonlinear regression using Polymath software. Since the regression analysis only had a mathematical basis, several contour conditions were imposed so that the kinetic parameters obtained could likewise be thermodynamically consistent. The different data for glycerol concentration in the outlet obtained in the OSR experiments at 923 K were fitted to exponential curves and reaction rates along the axial direction of the monolith were calculated by numerically differentiating the exponential fitting curves. To estimate the apparent activation energy for product formation, additional experiments were carried out at 823 and 873 K. According to the results obtained, the Equation 23 was proposed for the rate of consumption of glycerol:

$$(-r_G) = \frac{kP_G\sqrt{P_{H2O}}}{\left(1+K_GP_G+\sqrt{K_{H2O}P_{H2O}}\right)^2} \qquad \text{(Eq.23)}$$

Where k is the Arrenius-type kinetic constant, P_G the partial pressure of glycerol, P_{H2O} the partial pressure of steam, and K_G and K_{H2O} their corresponding adsorption equilibrium constants. Therefore, a reaction mechanism based on the non-dissociative adsorption of glycerol and the dissociative adsorption of steam was proposed, with the surface reaction being the rate

846 determining step in the LH mechanism. The estimated values for the kinetic parameters were
847 $k=0.110\ mol \cdot min^{-1} \cdot g^{-1} \cdot kPa^{-3/2}$ and $E_a=130.7\ kJ \cdot mol^{-1}$.
848
849 **6. Concluding remarks and future prospects**
850 Contrary to SR of glycerol, the OSR of glycerol has been considerably less studied. A possible
851 reason for that could be that most of the research in glycerol gasification has focused on hydrogen
852 production. However, hydrogen can be obtained by water electrolysis using renewable electricity,
853 (*e.g.*, photovoltaic energy) at estimated prices below 1€/kg by 2030-2040 considering the capital
854 (CAPEX) and operational (OPEX) expenditures [82].
855 Conversely, most of the materials and chemicals used in a daily basis need a carbon source for
856 their production. The production of syngas necessary for Gas-to-Liquids (GtL) technologies (such
857 as the Fischer-Tropsch synthesis and methanol-to-hydrocarbon processes) still needs to be
858 addressed to find sustainable, renewable, and cost-competitive alternatives to fossil resources.
859 In a GtL process, obtaining and conditioning the syngas is the most capital and energy intensive
860 part of the production plant, responsible for most of the energy requirements and for 50-75% of
861 the capital cost of the plant [83,84]. Therefore, efforts must be directed toward obtaining
862 renewable and cost-competitive alternatives for producing syngas. In this context, glycerol OSR
863 can play a key role in the transition from fossil-derived syngas to renewable-sourced. The
864 prospects for the world biodiesel market allow to conclude that crude glycerin surpluses may flood
865 the market in the next decade, and efforts to valorize these commodities and to offer alternative
866 proofs-of-concept for their exploitation will continue in the years to come.
867
868 Outcomes from literature can be summarized as follows:
869 1. The process parameters that have been explored typically are: $823 \geq T \geq 1123$ K, $S/C \leq 4$,
870 and $O/C \leq 1$.
871 2. The robustness of OSR is much higher than other reforming technologies, including the
872 most studied SR so far.
873 3. Several catalysts can work with low deactivation caused by carbon deposits, and some
874 can recover almost full activity by regeneration upon several hours on stream, even when
875 using crude glycerol.

4. The production of syngas by OSR is high in comparison with concurrent technologies, and $H_2/CO \simeq 2$ (ideal to produce methanol and Fischer-Tropsch synthesis) can be easily achieved by properly managing the O/C and S/C ratios in the feed. However, catalyst performance in long time-on-stream operation with high activity and stability should be considered when selecting the optimal operating conditions.
5. Interesting results have been obtained at lab-scale, though the scale-up of glycerol OSR is missing and should be addressed in further studies, in combination with technoeconomic assessment studies on the viability of scaled-up proofs-of-concept and pilot plants.
6. The thermodynamics of the process has been sufficiently covered and the available information reveals that syngas can be produced by OSR of glycerol in an energy-efficient and cost-competitive manner whilst achieving autothermal operation (ATR).
7. There is a significant lack of kinetic and mechanistic studies that could help gaining deeper insights into the glycerol OSR process. To date, only a few studies addressed this topic, and more research is needed to clearly understand the reaction mechanism in the different catalysts proposed. Mechanistic studies would help in the design of more robust and efficient catalysts for this process.
8. Novel concepts and reactor designs must be proposed for the development of OSR technology at larger scales. Considering that a prolonged catalyst lifetime is key to the technoeconomic viability of OSR technology at large scale, to preserve the catalyst lifetime by preventing deactivation by sintering, poisoning and carbon deposition is a must. In catalyst design, new formulations should be oriented to tune the product gases derived from glycerol non-catalytic decomposition, being capable of displaying high activity in reforming and WGS reactions and to selectively produce high quality syngas, ensuring stable operation (*i.e.*, without loss of activity) over extended periods of time. In addition, the study of different feeds having varying purity grades using this configuration could be of interest to determine which alternative is the best. Possibly, crude glycerol could be directly processed without needing any pre-conditioning or purification treatment. Furthermore, the analysis of these proofs-of-concept should include the

905 possibility of conducting the glycerol OSR at relevant operating pressures to avoid syngas
906 pressurization downstream.
907 9. The oxidizing environment of OSR is a clear setback for transition metals, which are more
908 prone to oxidation and thus to lose reforming activity over time. Therefore, efforts should
909 be directed to find new formulations, more resistant against oxidation, by the addition of
910 promoters that could establish difficult-to-oxidize alloys with the active phase based on
911 transition metals. In this sense, deeper insight on the use of Co as active phase is needed,
912 in view of its capacity for regeneration and reuse [69]. However, rational noble metals
913 formulations that could yield highly active and stable catalysts may offer a very interesting
914 possibility, provided that the load of the noble metal is minimized as much as possible for
915 economic and sustainability reasons.
916 10. Process intensification can help developing glycerol OSR at larger scales. Further studies
917 should explore different structured catalytic reactors, designs, and concepts. The dual-
918 layer concept offered interesting results, though a combination of non-catalytic glycerol
919 thermal decomposition and sequential catalytic processing using structured catalysts
920 may be a very interesting alternative, which can offer interesting possibilities benefitting
921 from its simplicity as concerns the formulation of the catalyst active layer. Thermal
922 stability, homogeneous layout and adherence of the catalytic layer are key requisites for
923 structured catalytic reactors. For this reason, new structured catalytic reactors should be
924 developed and tested in this process, with special attention to catalytic active layers that
925 could selectively transform product gases from the non-catalytic thermal decomposition
926 of glycerol into syngas with tuned H_2/CO ratios for the conceived downstream application.
927
928
929 **Acknowledgments**
930 António Portugal and Rui Moreira are grateful to the Portuguese Foundation for Science and
931 Technology (FCT) and the European Development Regional Fund (ERDF) for funding under the
932 scope of the MultiBiorefinery project (POCI-01-0145-FEDER-016403). J. Matheos and J. Arch
933 are gratefully acknowledged by Fernando Bimbela for the support provided during the preparation
934 of this manuscript. Luis M. Gandía thanks *Banco de Santander* and *Universidad Pública de*

Navarra for their financial support under the “Programa de Intensificación de la Investigación 2018” initiative. Fernando Bimbela and Luis M. Gandía wish to thank financial support from Spanish *Ministerio de Ciencia, Innovación y Universidades*, and the European Regional Development Fund (ERDF/FEDER) (grant RTI2018-096294-B-C31). José Luis Sánchez expresses his gratitude to Aragón Government (Ref. T22_20R), co-funded by FEDER 2014-2020 "*Construyendo Europa desde Aragón*" for providing frame support for this work.

The authors are grateful to Svend Ravn (Media Relation Manager | Corporate Communication) for kindly granting authorization for the use of the images in Figure 4 (Topsøe’s SynCOR™ technology) on the behalf of Haldor Topsøe Company, which is the owner of the copyrights.

Professor António Portugal deceased on 11th January 2021. Rui Moreira is deeply thankful to Professor António Portugal for his long-term friendship, PhD supervision and legacy. All the authors wholeheartedly miss Professor António Portugal.

Declaration of competing interests

The authors declare that they have no known competing for financial interests or personal relationships that could have appeared to influence the work reported in this paper.

Author contributions

Rui Moreira: Conceptualization, Writing - original draft, Writing - review & editing; **Fernando Bimbela**: Conceptualization, Writing - review & editing; **Luis M. Gandía**: Conceptualization, Writing - review & editing; **Abel Ferreira**: Writing - review & editing; **José Luis Sánchez**: Writing - review & editing, Validation; **António Portugal**: Funding acquisition, Project administration, Review and Validation.

References

[1] European Parliament; European Council. Directive 2009/28/EC on the promotion of the use of energy from renewable sources. Off J Eur Union 2009;140:16–62. https://doi.org/10.3000/17252555.L_2009.140.eng.

[2] European Parliament. Directive 2009/30/EC - amending Directive 98/70/EC as regards the specification of petrol, diesel and gas-oil and introducing a mechanism to monitor and reduce greenhouse gas emissions. Off J Eur Union 2009:88–113.

[3] European Parliament. Directive 98/70/EC of the European Parliament and of the Council of 13 October 1998 relating to the quality of petrol and diesel fuels and amending Council Directive 93/12/EEC [1998] OJ L 350. Off J Eur Union 2011:1–41.

[4] European Parliament. Directive 2015/1513 of the European Parliament and of the Council. Off J Eur Union 2015;L239:1–29. https://doi.org/http://eur-lex.europa.eu/pri/en/oj/dat/2003/l_285/l_28520031101en00330037.pdf.

[5] OECD/FAO. OECD-FAO Agricultural Outlook. 2015. https://doi.org/10.1787/agr-outl-data-en.

[6] OECD/FAO. OECD-FAO Agricultural Outlook 2019-2028. OECD publishing; 2019. https://doi.org/10.1787/agr_outloook-2019-en.

[7] Talavera-Prieto NMC, Ferreira AGM, Moreira RJ, Portugal ATG. Monitoring of the transesterification reaction by continuous off-line density measurements. Fuel 2020;264:116877. https://doi.org/10.1016/j.fuel.2019.116877.

[8] Prieto NMCT, Ferreira AGM, Portugal ATG, Moreira RJ, Santos JB. Correlation and prediction of biodiesel density for extended ranges of temperature and pressure. Fuel 2015;141:23–38. https://doi.org/10.1016/j.fuel.2014.09.113.

[9] Nguyen TTNN, Bellière-Baca V, Rey P, Millet JMMM. Efficient catalysts for simultaneous dehydration of light alcohols in gas phase. Catal Sci Technol 2015;5:3576–84. https://doi.org/10.1039/C5CY00306G.

[10] Takkellapati S, Li T, Gonzalez MA. An overview of biorefinery-derived platform chemicals from a cellulose and hemicellulose biorefinery. Clean Technol Environ Policy 2018;20:1615–30. https://doi.org/10.1007/s10098-018-1568-5.

[11] Haveren J van, Scott EL, Sanders J. Bulk chemicals from biomass. Biofuels, Bioprod Biorefining 2008;2:41–57. https://doi.org/10.1002/bbb.43.

[12] Choi S, Song CW, Shin JH, Lee SY. Biorefineries for the production of top building block chemicals and their derivatives. Metab Eng 2015;28:223–39. https://doi.org/10.1016/j.ymben.2014.12.007.

[13] Lin YC. Catalytic valorization of glycerol to hydrogen and syngas. Int J Hydrogen Energy 2013;38:2678–700. https://doi.org/10.1016/j.ijhydene.2012.12.079.

[14] Quispe CAG, Coronado CJR, Carvalho Jr. JA. Glycerol: Production, consumption, prices, characterization and new trends in combustion. Renew Sustain Energy Rev 2013;27:475–93. https://doi.org/10.1016/j.rser.2013.06.017.

[15] Anufriev IS. Review of water/steam addition in liquid-fuel combustion systems for NO_x reduction: Waste-to-energy trends. Renew Sustain Energy Rev 2021;138:110665. https://doi.org/10.1016/j.rser.2020.110665.

[16] Gruca M, Pyrc M, Szwaja M, Szwaja S. Effective Combustion of Glycerol in a Compression Ignition Engine Equipped with Double Direct Fuel Injection. Energies 2020;13:6349. https://doi.org/10.3390/en13236349.

[17] Presciutti A, Asdrubali F, Baldinelli G, Rotili A, Malavasi M, Di Salvia G. Energy and exergy analysis of glycerol combustion in an innovative flameless power plant. J Clean Prod 2018;172:3817–24. https://doi.org/10.1016/j.jclepro.2017.06.022.

[18] Bohon MD, Metzger BA, Linak WP, King CJ, Roberts WL. Glycerol combustion and emissions. Proc Combust Inst 2011;33:2717–24. https://doi.org/10.1016/j.proci.2010.06.154.

[19] Steinmetz SA, Herrington JS, Winterrowd CK, Roberts WL, Wendt JOL, Linak WP. Crude glycerol combustion: Particulate, acrolein, and other volatile organic emissions. Proc Combust Inst 2013;34:2749–57. https://doi.org/10.1016/j.proci.2012.07.050.

[20] Reuss G, Disteldorf W, Gamer AO, Hilt A. Formaldehyde. Ullmann's Encycl. Ind. Chem., Weinheim, Germany: Wiley-VCH Verlag GmbH & Co. KGaA; 2005, p. 1–34. https://doi.org/10.1002/14356007.a11_619.

[21] Kohlpaintner C, Schulte M, Falbe J, Lappe P, Weber J. Aldehydes, Aliphatic and Araliphatic. Ullmann's Encycl. Ind. Chem., Weinheim, Germany: Wiley-VCH Verlag GmbH & Co. KGaA; 2005, p. 1–35. https://doi.org/10.1002/14356007.a01_321.

[22] Reutemann W, Kieczka H. Formic Acid. Ullmann's Encycl. Ind. Chem., Weinheim, Germany: Wiley-VCH Verlag GmbH & Co. KGaA; 2005, p. 1–21. https://doi.org/10.1002/14356007.a12_013.

[23] Cheung H, Tanke RS, Torrence GP. Acetic Acid. Ullmann's Encycl. Ind. Chem., Weinheim, Germany: Wiley-VCH Verlag GmbH & Co. KGaA; 2000, p. 1–30. https://doi.org/10.1002/14356007.a01_045.

[24] Leonzio G. State of art and perspectives about the production of methanol, dimethyl ether and syngas by carbon dioxide hydrogenation. J CO_2 Util 2018;27:326–54. https://doi.org/10.1016/j.jcou.2018.08.005.

[25] Fiedler E, Grossmann G, Kersebohm DB, Weiss G, Witte C. Methanol. Ullmann's Encycl. Ind. Chem., Weinheim, Germany: Wiley-VCH Verlag GmbH & Co. KGaA; 2005, p. 1–25. https://doi.org/10.1002/14356007.a16_465.

[26] Ilias S, Bhan A. Mechanism of the catalytic conversion of methanol to hydrocarbons. ACS Catal 2013;3:18–31. https://doi.org/10.1021/cs3006583.

[27] Mokrani T, Scurrell M. Gas Conversion to Liquid Fuels and Chemicals: The Methanol Route-Catalysis and Processes Development. Catal Rev 2009;51:1–145. https://doi.org/10.1080/01614940802477524.

[28] Roslan NA, Abidin SZ, Ideris A, Vo DVN. A review on glycerol reforming processes over Ni-based catalyst for hydrogen and syngas productions. Int J Hydrogen Energy 2020;45:18466–89. https://doi.org/10.1016/j.ijhydene.2019.08.211.

[29] Kulagin VA, Grushevenko DA. Will Hydrogen Be Able to Become the Fuel of the Future? Therm Eng 2020;67:189–201. https://doi.org/10.1134/S0040601520040023.

[30] Bac S, Keskin S, Avci AK. Recent advances in materials for high purity H_2 production by ethanol and glycerol steam reforming. Int J Hydrogen Energy 2020;45:34888–917. https://doi.org/10.1016/j.ijhydene.2019.11.237.

[31] Ambursa MM, Juan JC, Yahaya Y, Taufiq-Yap YH, Lin YC, Lee HV. A review on catalytic hydrodeoxygenation of lignin to transportation fuels by using nickel-based catalysts. Renew Sustain Energy Rev 2021;138:110667. https://doi.org/10.1016/j.rser.2020.110667.

[32] Abidin SZ, Ideris A, Ainirazali N, Ismail M. A Short Review on Production of Syngas via Glycerol Dry Reforming. In: Inamuddin, Asiri AM, Lichtfouse E, editors. Convers. Carbon Dioxide

into Hydrocarb. Vol. 2 Technol., Cham: Springer International Publishing; 2020, p. 185–97. https://doi.org/10.1007/978-3-030-28638-5_7.

[33] Yu J, Odriozola JA, Reina TR. Dry Reforming of Ethanol and Glycerol: Mini-Review. Catalysts 2019;9:1015. https://doi.org/10.3390/catal9121015.

[34] Tamošiūnas A, Gimžauskaitė D, Uscila R, Aikas M. Thermal arc plasma gasification of waste glycerol to syngas. Appl Energy 2019;251. https://doi.org/10.1016/j.apenergy.2019.113306.

[35] Wang M, Liu M, Lu J, Wang F. Photo splitting of bio-polyols and sugars to methanol and syngas. Nat Commun 2020;11:1–9. https://doi.org/10.1038/s41467-020-14915-8.

[36] Schwengber CA, Alves HJ, Schaffner RA, Da Silva FA, Sequinel R, Bach VR, et al. Overview of glycerol reforming for hydrogen production. Renew Sustain Energy Rev 2016;58:259–66. https://doi.org/10.1016/j.rser.2015.12.279.

[37] Davda RR, Shabaker JW, Huber GW, Cortright RD, Dumesic JA. A review of catalytic issues and process conditions for renewable hydrogen and alkanes by aqueous-phase reforming of oxygenated hydrocarbons over supported metal catalysts. Appl Catal B Environ 2005;56:171–86. https://doi.org/10.1016/j.apcatb.2004.04.027.

[38] Adhikari S, Fernando SD, Haryanto A. Hydrogen production from glycerol: An update. Energy Convers Manag 2009;50:2600–4. https://doi.org/10.1016/j.enconman.2009.06.011.

[39] Haynes DJ, Shekhawat D. Oxidative Steam Reforming. Fuel Cells Technol. Fuel Process., Elsevier; 2011, p. 129–90. https://doi.org/10.1016/B978-0-444-53563-4.10006-9.

[40] Moral A, Reyero I, Llorca J, Bimbela F, Gandía LM. Partial oxidation of methane to syngas using Co/Mg and Co/Mg-Al oxide supported catalysts. Catal Today 2019;333:259–67. https://doi.org/10.1016/j.cattod.2018.04.003.

[41] Rostrup-Nielsen JR. An industrial perspective on the impact of Haldor Topsøe on research and development in synthesis gas production. J Catal 2015;328:5–10. https://doi.org/10.1016/j.jcat.2015.04.013.

[42] Topsoe. Syncor Auto-Thermal Reforming n.d. https://www.topsoe.com/products/equipment/syncortm-autothermal-reformer-atr?hsLang=en (accessed September 11, 2020).

[43] Dybkjaer I. Tubular reforming and autothermal reforming of natural gas — an overview of available processes. Fuel Process Technol 1995;42:85–107. https://doi.org/10.1016/0378-3820(94)00099-F.

[44] Aasberg-Petersen K, Bak Hansen J-H, Christensen T., Dybkjaer I, Christensen PS, Stub Nielsen C, et al. Technologies for large-scale gas conversion. Appl Catal A Gen 2001;221:379–87. https://doi.org/10.1016/S0926-860X(01)00811-0.

[45] Rennard DC, Kruger JS, Schmidt LD. Autothermal catalytic partial oxidation of glycerol to syngas and to non-equilibrium products. ChemSusChem 2009;2:89–98. https://doi.org/10.1002/cssc.200800200.

[46] Rennard DC, Kruger JS, Michael BC, Schmidt LD. Long-time behavior of the catalytic partial oxidation of glycerol in an autothermal reactor. Ind Eng Chem Res 2010;49:8424–32. https://doi.org/10.1021/ie100405h.

[47] Liu Y, Farrauto R, Lawal A. Autothermal reforming of glycerol in a dual layer monolith catalyst. Chem Eng Sci 2013;89:31–9. https://doi.org/10.1016/j.ces.2012.11.030.

[48] Liu Y, Lawal A. Kinetic study of autothermal reforming of glycerol in a dual layer monolith catalyst. Chem Eng Process Process Intensif 2015;95:276–83. https://doi.org/10.1016/j.cep.2015.07.008.

[49] Liu Y, Lawal A. Thermodynamic Analysis and Characterization of Syngas Production by Autothermal Reforming of Biodiesel Byproducts. Energy Technol 2014;2:792–801. https://doi.org/10.1002/ente.201402080.

[50] Gutiérrez Ortiz FJ, Ollero P, Serrera A, Galera S. Autothermal Reforming of Glycerol with Supercritical Water for Maximum Power through a Turbine Plus a Fuel Cell. Energy & Fuels 2013;27:576–87. https://doi.org/10.1021/ef301509n.

[51] Jimmy U, Mohamedali M, Ibrahim H. Thermodynamic Analysis of Autothermal Reforming of Synthetic Crude Glycerol (SCG) for Hydrogen Production. ChemEngineering 2017;1:4. https://doi.org/10.3390/chemengineering1010004.

[52] Wang H, Wang X, Li M, Li S, Wang S, Ma X. Thermodynamic analysis of hydrogen production from glycerol autothermal reforming. Int J Hydrogen Energy 2009;34:5683–90. https://doi.org/10.1016/j.ijhydene.2009.05.118.

[53] Bimbela F, Oliva M, Ruiz J, García L, Arauzo J. Hydrogen production via catalytic steam reforming of the aqueous fraction of bio-oil using nickel-based coprecipitated catalysts. Int J Hydrogen Energy 2013;38:14476–87. https://doi.org/10.1016/j.ijhydene.2013.09.038.

[54] Bimbela F, Oliva M, Ruiz J, García L, Arauzo J. Hydrogen production by catalytic steam reforming of acetic acid, a model compound of biomass pyrolysis liquids. J Anal Appl Pyrolysis 2007;79:112–20. https://doi.org/10.1016/j.jaap.2006.11.006.

[55] Bimbela F, Oliva M, Ruiz J, García L, Arauzo J. Catalytic steam reforming of model compounds of biomass pyrolysis liquids in fixed bed: Acetol and n-butanol. J Anal Appl Pyrolysis 2009;85:204–13. https://doi.org/10.1016/j.jaap.2008.11.033.

[56] Authayanun S, Arpornwichanop A, Paengjuntuek W, Assabumrungrat S. Thermodynamic study of hydrogen production from crude glycerol autothermal reforming for fuel cell applications. Int J Hydrogen Energy 2010;35:6617–23. https://doi.org/10.1016/j.ijhydene.2010.04.050.

[57] Yang G, Yu H, Peng F, Wang H, Yang J, Xie D. Thermodynamic analysis of hydrogen generation via oxidative steam reforming of glycerol. Renew Energy 2011;36:2120–7. https://doi.org/10.1016/j.renene.2011.01.022.

[58] Hajjaji N, Baccar I, Pons MN. Energy and exergy analysis as tools for optimization of hydrogen production by glycerol autothermal reforming. Renew Energy 2014;71:368–80. https://doi.org/10.1016/j.renene.2014.05.056.

[59] Leal AL, Soria MA, Madeira LM. Autothermal reforming of impure glycerol for H_2 production: Thermodynamic study including in situ CO_2 and/or H_2 separation. Int J Hydrogen Energy 2016;41:2607–20. https://doi.org/10.1016/j.ijhydene.2015.11.132.

[60] Swami SM, Abraham MA. Integrated catalytic process for conversion of biomass to hydrogen. Energy and Fuels 2006;20:2616–22. https://doi.org/10.1021/ef060054f.

[61] Douette AMD, Turn SQ, Wang W, Keffer VI. Experimental investigation of hydrogen production from glycerin reforming. Energy and Fuels 2007;21:3499–504. https://doi.org/10.1021/ef060379w.

[62] Kamonsuangkasem K, Therdthianwong S, Therdthianwong A. Hydrogen production from yellow glycerol via catalytic oxidative steam reforming. Fuel Process Technol 2013;106:695–703. https://doi.org/10.1016/j.fuproc.2012.10.003.

1134 [63] Lin KH, Chang ACC, Lin WH, Chen SH, Chang CY, Chang HF. Autothermal steam
1135 reforming of glycerol for hydrogen production over packed-bed and Pd/Ag alloy membrane
1136 reactors. Int J Hydrogen Energy 2013;38:12946–52.
1137 https://doi.org/10.1016/j.ijhydene.2013.04.134.
1138 [64] Sadykov V, Mezentseva N, Fedorova Y, Lukashevich A, Pelipenko V, Kuzmin V, et al.
1139 Structured catalysts for steam/autothermal reforming of biofuels on heat-conducting substrates:
1140 Design and performance. Catal Today 2015;251:19–27.
1141 https://doi.org/10.1016/j.cattod.2014.10.045.
1142 [65] Sadykov V, Mezentseva N, Simonov M, Smal E, Arapova M, Pavlova S, et al. Structured
1143 nanocomposite catalysts of biofuels transformation into syngas and hydrogen: Design and
1144 performance. Int J Hydrogen Energy 2015;40:7511–22.
1145 https://doi.org/10.1016/j.ijhydene.2014.11.151.
1146 [66] Sabri F, Idem R, Ibrahim H. Metal oxide-based catalysts for the autothermal reforming of
1147 glycerol. Ind Eng Chem Res 2018;57:2486–97. https://doi.org/10.1021/acs.iecr.7b04582.
1148 [67] Abdul Ghani A, Torabi F, Ibrahim H. Autothermal reforming process for efficient hydrogen
1149 production from crude glycerol using nickel supported catalyst: Parametric and statistical
1150 analyses. Energy 2018;144:129–45. https://doi.org/10.1016/j.energy.2017.11.132.
1151 [68] Koc S, Avci AK. Reforming of glycerol to hydrogen over Ni-based catalysts in a
1152 microchannel reactor. Fuel Process Technol 2017;156:357–65.
1153 https://doi.org/10.1016/j.fuproc.2016.09.019.
1154 [69] Moreira R, Moral A, Bimbela F, Portugal A, Ferreira A, Sanchez JL, et al. Syngas
1155 production via catalytic oxidative steam reforming of glycerol using a Co/Al coprecipitated catalyst
1156 and different bed fillers. Fuel Process Technol 2019;189:120–33.
1157 https://doi.org/10.1016/j.fuproc.2019.02.014.
1158 [70] Veiga S, Romero M, Faccio R, Segobia D, Duarte H, Apesteguía C, et al. Hydrogen-rich
1159 gas production by steam and oxidative steam reforming of crude glycerol over Ni-La-Me mixed
1160 oxide catalysts (Me = Ce and/or Zr). Catal Today 2020;344:190–8.
1161 https://doi.org/10.1016/j.cattod.2019.02.008.

[71] Liu SK, Lin YC. Generation of syngas through autothermal partial oxidation of glycerol over $LaMnO_3$- and $LaNiO_3$-coated monoliths. Catal Today 2014;237:62–70. https://doi.org/10.1016/j.cattod.2013.12.028.

[72] Lin KH, Lin WH, Hsiao CH, Chang HF, Chang ACC. Hydrogen production in steam reforming of glycerol by conventional and membrane reactors. Int J Hydrogen Energy 2012;37:13770–6. https://doi.org/10.1016/j.ijhydene.2012.03.111.

[73] Dauenhauer PJ, Salge JR, Schmidt LD. Renewable hydrogen by autothermal steam reforming of volatile carbohydrates. J Catal 2006;244:238–47. https://doi.org/10.1016/j.jcat.2006.09.011.

[74] Liu SK, Lin YC. Autothermal partial oxidation of glycerol to syngas over Pt-, $LaMnO_3$-, and Pt/$LaMnO_3$-coated monoliths. Ind Eng Chem Res 2012;51:16278–87. https://doi.org/10.1021/ie3021686.

[75] Delparish A, Koc S, Caglayan BS, Avci AK. Oxidative steam reforming of glycerol to synthesis gas in a microchannel reactor. Catal Today 2019;323:200–8. https://doi.org/10.1016/j.cattod.2018.03.047.

[76] Ayoobi M, Schoegl I. Non-catalytic conversion of glycerol to syngas at intermediate temperatures: Numerical methods with detailed chemistry. Fuel 2017;195:190–200. https://doi.org/10.1016/j.fuel.2017.01.065.

[77] Abdul Ghani A, Torabi F, Ibrahim H. Kinetics of hydrogen production by the autothermal reforming of crude glycerol over modified nickel supported catalyst. J Environ Chem Eng 2017;5:5827–35. https://doi.org/10.1016/j.jece.2017.11.022.

[78] Afabor E, Salama A, Ibrahim H. Packed bed reactor modeling of the catalytic auto-thermal reforming of synthetic crude glycerol. J Environ Chem Eng 2017;5:4850–7. https://doi.org/10.1016/j.jece.2017.09.016.

[79] Sabri F, Bakhtiari M, Ibrahim H. Robust power-law kinetic model for the autothermal reforming of glycerol over metal oxide catalysts. React Kinet Mech Catal 2018;123:543–57. https://doi.org/10.1007/s11144-017-1337-1.

[80] Hwang HS, Farrauto RJ. Process for generating hydrogen-rich gas, 2005.

[81] De Vrieze J, Verbeeck K, Pikaar I, Boere J, Van Wijk A, Rabaey K, et al. The hydrogen gas bio-based economy and the production of renewable building block chemicals, food and energy. N Biotechnol 2020;55:12–8. https://doi.org/10.1016/j.nbt.2019.09.004.

[82] Dybkjær I, Christensen TS. Syngas for Large Scale Conversion of Natural Gas to Liquid Fuels. Stud. Surf. Sci. Catal., vol. 136, 2001, p. 435–40. https://doi.org/10.1016/S0167-2991(01)80342-6.

[83] Aasberg-Petersen K, Christensen TS, Stub Nielsen C, Dybkjær I. Recent developments in autothermal reforming and pre-reforming for synthesis gas production in GTL applications. Fuel Process Technol 2003;83:253–61. https://doi.org/10.1016/S0378-3820(03)00073-0.